ESAIM: M2AN 55 (2021) 913–938
https://doi.org/10.1051/m2an/2021012

ESAIM: Mathematical Modelling and Numerical Analysis
www.esaim-m2an.org

AN EFFICIENT VARIABLE STEP-SIZE METHOD FOR OPTIONS PRICING UNDER JUMP-DIFFUSION MODELS WITH NONSMOOTH PAYOFF FUNCTION

Wansheng Wang*, Mengli Mao and Zheng Wang

Abstract. We develop an implicit–explicit midpoint formula with variable spatial step-sizes and variable time step to solve parabolic partial integro-differential equations with nonsmooth payoff function, which describe the jump-diffusion option pricing model in finance. With spatial differential operators being treated by using finite difference methods and the jump integral being computed by using the composite trapezoidal rule on a non-uniform space grid, the proposed method leads to linear systems with tridiagonal coefficient matrices, which can be solved efficiently. Under realistic regularity assumptions on the data, the consistency error and the global error bounds for the proposed method are obtained. The stability of this numerical method is also proved by using the Von Neumann analysis. Numerical results illustrate the effectiveness of the proposed method for European options under jump-diffusion models.

Mathematics Subject Classification. 65M06, 65M55, 65L60, 91B25, 91G60, 65J10.

Received May 2, 2020. Accepted March 11, 2021.

1. Introduction

In this paper, we propose an implicit–explicit (IMEX) time discretization method in combination with a finite difference method in space for solving parabolic integro-differential equations (PIDEs), which arise in asset pricing problems in mathematical finance,

$$\frac{\partial u(\tau,x)}{\partial \tau} = \mathcal{L}u(\tau,x) + \mathcal{I}u(\tau,x), \quad (\tau,x) \in (0,T] \times \Omega, \tag{1.1}$$

$$u(0,x) = g(x), \quad x \in \Omega, \tag{1.2}$$

containing a differential operator $\mathcal{L}$ and a nonlocal integral operator $\mathcal{I}$,

$$\mathcal{L}u(\tau,x) = \frac{1}{2}\sigma^2 \frac{\partial^2 u}{\partial x^2} + \left(r - \frac{1}{2}\sigma^2 - \lambda\kappa\right)\frac{\partial u}{\partial x} - (r+\lambda)u, \tag{1.3}$$

$$\mathcal{I}u(\tau,x) = \lambda \int_{\mathbb{R}} u(\tau, x+y) f(y) \mathrm{d}y, \tag{1.4}$$

Keywords and phrases. Partial integro-differential equations, implicit–explicit midpoint formula, options pricing, jump-diffusion model, finite difference method, stability, error estimates.

Department of Mathematics, Shanghai Normal University, Shanghai 200234, P.R. China.
*Corresponding author: w.s.wang@163.com

Article published by EDP Sciences

where the domain $\Omega := (X_l, X_r)$ with a sufficiently small X_l and a sufficiently large X_r will be chosen appropriately and the initial function $g(x)$ derives from the payoff function for the option contract. The parameters r, σ, λ, κ and function f will be specialized in the next section. As pointed out in [27, 36, 55], for almost all financial model problems, the given payoff function $g(x)$ is nonsmooth and singularities may arise at $\tau = 0$. Consequently, two main problems in numerical analysis and implement of numerical methods for this class of equations confront with are the non-locality of the integral operator $\mathcal{I}$ and the non-smoothness of the payoff function $g(x)$.

The standard finite difference scheme is the most common way to discretize the differential operators in the option pricing context (see, *e.g.*, [1, 49]). When an implicit time stepping scheme is used to approximate the time derivative, the discretization of the nonlocal integral operator $\mathcal{I}$ with standard finite difference scheme will produce dense systems with full matrices. In numerically solving jump-diffusion models, one of the greatest challenges is how to reduce the computational cost. On the one hand, to solve the resulting systems with full matrices, some algorithms such as alternating direct implicit (ADI) methods (see, *e.g.*, [4, 25]), FFT [3, 19], iterative methods [3, 18, 44, 49, 50], and multigrid methods [12, 53], have already been designed. On the other hand, to avoid the inversion of a full matrix, the IMEX time discretizations that treat typically the nonlocal integral operator $\mathcal{I}$ explicitly and the rest of the operators implicitly are exploited as an increasingly popular alternative. To the best of our knowledge, IMEX schemes were first introduced by Crouzeix [17] and Varah [51] and then analyzed by many numerical mathematicians (for early literatures, see, *e.g.*, [2, 5, 6, 22, 43, 52]). Research on the IMEX schemes for pricing option under jump-diffusion model has recently become very active (see, *e.g.*, [9, 10, 13, 16, 20, 23, 25, 27, 29, 34, 40–42, 45, 46, 49, 57, 58]), since the resulting tridiagonal systems can be solved directly and extremely efficiently.

We note that these IMEX schemes analyzed in the literature are based on the uniform time grid. However, since the non-smoothness of the payoff function $g(x)$ may leads to singularities of the solution at $\tau = 0$, variable time grids are needed for solving the option pricing model (1.1) and (1.2). To study the variable time-stepping schemes, the analyticity property of the solution to PIDEs (1.1) and (1.2) arising in finance should be investigated. This was first exploited for the space semi-discrete parabolic problem in [36], and the so-called geometric time grids are used to resolve the low regularity of the solution at $\tau = 0$ for the *hp*-discontinuous Galerkin time-stepping scheme. The L^∞ regularity of the solution to PIDEs (1.1) and (1.2) was further analyzed in [16], and a constant step-size IMEX Euler finite difference scheme is used to solve this class of option pricing problem. In [55], the L^2 time regularity of the solution to abstract PIDEs was investigated, and the stability and convergence of the variable step-size IMEX two-step backward differentiation formula (BDF2) for solving PIDEs (1.1) and (1.2) were shown by energy method based on their time regularity results. We find that the only disadvantage of the variable step-size IMEX BDF2 scheme is that the upper bound of its step-size ratios is subject to a constant (see, *e.g.*, [11, 35, 55, 56]). Although our time grids will generally satisfy the bound in practical applications, it's not perfect theoretically. In this paper, we thus study the variable step-size IMEX midpoint (MP) formula, which is closely related to the Crank–Nicolson-Leapfrog (CNLF) scheme, for solving the financial model (1.1) and (1.2), and show that its step-size ratios are not subject to such a bound. In addition, different from [55], we show the stability of variable step-size IMEX MP method together with variable spatial step-sizes finite difference method for this model by using the Von Neumann analysis, and derive the discrete l^2 error bounds for this fully discrete method for nonsmooth payoff function based on the L^∞ regularity of the solution obtained in [16].

To accomplish these, in Section 2, we introduce mathematical models for option pricing problems under jump-diffusion process. In Section 3, we combine a finite difference scheme for spatial variable step-size discretization with the variable step-size IMEX MP method for time discretization for solving this class of model problems. A numerical study is carried out for European Merton' and Kou' models in Section 4, compared with the variable step-size IMEX BDF2 scheme. The stability of this scheme is proved in Section 5. To obtain the error estimates for this scheme, some assumptions, which are satisfied for these model problems considered here, are made on the integral operator and the payoff function in Section 6. Then, in this section, the consistency error and the

global error bounds are derived based on L^∞ regularity lemma obtained in [16]. The paper ends with conclusions in Section 7.

2. Jump-diffusion models under Lévy processes

Parabolic problems of type (1.1) and (1.2) arise in finance in the problem of option pricing. To explain the market prices of options with various strike prices and maturities, some researchers considered the class of jump-diffusion models: the risk-neutral dynamics of the underlying asset is given by

$$S_t = S_0 \exp(rt + X_t), \tag{2.1}$$

where S_0 is the stock price at $t = 0$, r is interest rate, and X_t is a time-homogeneous jump-diffusion (Lévy) process.

2.1. Lévy processes and exponential Lévy models

A process $(X_t)_{t\geq 0}$ defined on a probability space $(\Omega, \mathcal{F}, \mathbb{P})$ is said to be a Lévy process if it possesses the following properties (see, *e.g.*, [15,47]):

(i) The paths of X_t are $\mathbb{P}$-almost surely right continuous with left limits.
(ii) $\mathbb{P}(X_0 = 0) = 1$.
(iii) For $0 \leq s \leq t$, $X_t - X_s$ is equal in distribution to X_{t-s}.
(iv) For $0 \leq s \leq t$, $X_t - X_s$ is independent of $\{X_v : v \leq s\}$.

In general neither the marginal nor the incremental distribution of a Lévy process is given explicitly. However at the level of marginals Lévy process can be identified by their characteristic functions given by the so-called Lévy–Khintchine formula [47]:

$$\mathbb{E}\left[e^{izX_t}\right] = e^{-t\psi(z)} = \exp\left\{t\left(-\frac{\sigma^2 z^2}{2} + i\gamma z + \int_{\mathbb{R}} (e^{izx} - 1 - izx1_{|x|\leq 1})\nu(\mathrm{d}x)\right)\right\}, \tag{2.2}$$

where σ and γ are real constants, 1_Q is the indicator function with respect to a set Q, and ν is a Lévy measure on $\mathbb{R}$ satisfying both $\nu(\{0\}) = 0$ and

$$\int_{\mathbb{R}} \min(1, \mathrm{d}x)\nu(\mathrm{d}x) < \infty.$$

The triple of components (σ, γ, ν) is called the characteristic triple of $(X_t)_{t\geq 0}$ with σ denoting the diffusion component of the Lévy process.

Let $(S_t)_{t\in[0,T]}$ be the price of a financial asset modelled as a stochastic process on a filtered probability space $(\Omega, \mathcal{F}, \mathcal{F}_t, \mathbb{P})$ with filtration $\mathcal{F}_t$. With the representation (2.1), different exponential Lévy models proposed in the financial modelling literature simply correspond to different choices for the Lévy measure ν (see, *e.g.*, [15]). The classical Merton model [38] is based on a drifted Brownian motion with finitely many jumps, *i.e.*,

$$X_t := \sigma W_t + \sum_{i=1}^{N_t} Y_i, \tag{2.3}$$

where Y_i are independent and identically distributed random variables with distribution function $f(x)$, N_t is a Poisson process with intensity λ. In this classical model, the Lévy measure is given by $\nu(\mathrm{d}x) = k(x)\mathrm{d}x$ with $k(x) = \lambda f(x)$. In the model originally presented by Merton [38] the probability density function of the jump is given by

$$f(x) = \frac{1}{\sqrt{2\pi}\sigma_{\mathrm{Me}}} e^{-[x-\mu_{\mathrm{Me}}]^2/2\sigma_{\mathrm{Me}}^2}, \tag{2.4}$$

i.e., f is the normal distribution with mean μ_{Me} and standard deviation σ^2_{Me}. When the density function $f(x)$ has the form

$$f(x) = a\eta_1 e^{-\eta_1 x} 1_{x\geq 0} + b\eta_2 e^{\eta_2 x} 1_{x<0}, \tag{2.5}$$

where $\eta_1 > 1$, $\eta_2 > 0$, $a > 0$, and $b = 1 - a$, the financial model becomes the Kou's jump-diffusion model [31] in which Y_i follow an asymmetric double exponential distribution.

2.2. Partial integro-differential equation

For a given payoff $\phi(S)$, the value of the European option $V(t, S)$ at $S = S_t$ with maturity T can be expressed by the following discounted conditional expectation under the risk-adjusted martingale measure (sometimes called risk-neutral probability) $\mathbb{Q}$:

$$V(t, S) = \mathbb{E}\left[e^{-r(T-t)}\phi(S_T)|S_t = S\right]. \tag{2.6}$$

Note that under the hypothesis of no-arbitrage such a martingale measure $\mathbb{Q}$ equivalent to $\mathbb{P}$ exists. Applying Itô's formula and the principle of no-arbitrage one can show that V defined in (2.6) solves the PIDE (see, *e.g.*, [16, 39])

$$\frac{\partial V}{\partial t} + \frac{1}{2}\sigma^2 S^2 \frac{\partial^2 V}{\partial S^2} + rS\frac{\partial V}{\partial S} - rV + \int_{\mathbb{R}} \left(V(t, Se^y) - V - S(e^y - 1)\frac{\partial V}{\partial S}\right)\nu(\mathrm{d}y) = 0, \quad t \in (0, T], \tag{2.7}$$

on $[0, T) \times (0, \infty)$ with the terminal condition

$$V(T, S) = \phi(S), \quad S \in [0, \infty).$$

When we assume that the Lévy measure $\nu(\mathbb{R}) = \lambda < \infty$, the integral term in (2.7) can be split into three terms. Then by making the changes of variables $x = \ln(S/S_0)$, $\tau = T - t$, $V(T - t, S_0e^x) = U(\tau, x)$, evaluation of the option values requires solving the PIDE

$$\begin{aligned}\frac{\partial U}{\partial \tau} &= \frac{1}{2}\sigma^2\frac{\partial^2 U}{\partial x^2} + \left(r - \frac{1}{2}\sigma^2 - \lambda\kappa\right)\frac{\partial U}{\partial x} - (r + \lambda)U \\ &\quad + \lambda\int_{\mathbb{R}} U(\tau, x + y)f(y)\mathrm{d}y, \quad (\tau, x) \in (0, T] \times \mathbb{R}, \end{aligned} \tag{2.8}$$

$$U(0, x) = g(x), \quad x \in \mathbb{R}, \tag{2.9}$$

where $\kappa = \int_{\mathbb{R}}(e^x - 1)f(x)\mathrm{d}x$ and $g(x) = \phi(e^x)$. The boundary conditions will be different for different option pricing problems. In the case of European option, the boundary conditions are given by, for the call option

$$\lim_{x\to-\infty} U(\tau, x) = 0, \quad \text{and} \quad \lim_{x\to+\infty} U(\tau, x) = S_0e^x - Ke^{-r\tau} := \xi_1(\tau, x), \tag{2.10}$$

and, for the put option

$$\lim_{x\to-\infty} U(\tau, x) = Ke^{-r\tau} - S_0e^x := \xi_2(\tau, x), \quad \text{and} \quad \lim_{x\to+\infty} U(\tau, x) = 0, \tag{2.11}$$

where K is the strike price.

3. Fully discrete approximation of jump-diffusion models

In this section, we consider the fully discrete approximation of (2.8) and (2.9).

3.1. Localization to a bounded domain

To construct a numerical scheme for approximation of the PIDE (2.8) and (2.9), we first truncate the infinite domain $\mathbb{R}$ for x to be $\Omega := (X_l, X_r)$ with a sufficiently small X_l and a sufficiently large X_r. Taking into account the asymptotic behavior of the price of an option such as (2.10) and (2.11), on the truncated domain Ω, we solve the PIDE (1.1) and (1.2) with boundary conditions

$$u(\tau, x) = \xi(\tau, x), \quad x \in (X_l, X_r), \tag{3.1}$$

where $\xi = 0$ or $\xi = \xi_i$, $i = 1, 2$, depending on the option problem. If ξ is bounded ($\|\xi\|_{L^\infty} < \infty$) and there exists a constant $\varrho > 0$ such that $\int_{|x|>1} e^{\varrho|x|}\nu(\mathrm{d}x) < \infty$, the localization error $U(\tau, x) - u(\tau, x)$ has been estimated by Cont and Voltchkova in [16]:

$$|U(\tau, x) - u(\tau, x)| \le C_{\tau,\varrho}\|\xi\|_{L^\infty} e^{-\varrho(X-|x|)}, \quad \forall x \in (X_l, X_r) = (-X, X), \tag{3.2}$$

where the constant $C_{\tau,\varrho}$ is independent of X. The estimate (3.2) implies that the localization error decreases uniformly on each closed subinterval of $(-X, X)$. An L^2-norm estimate for the localization error is also given in [37] using analytical methods.

3.2. Finite difference discretization of spatial derivatives

Here we describe the discretization of the spatial derivative terms, that is, the operator

$$\mathcal{L}u(\tau, x) = \frac{1}{2}\sigma^2\frac{\partial^2 u}{\partial x^2} + \left(r - \frac{1}{2}\sigma^2 - \lambda\kappa\right)\frac{\partial u}{\partial x} - (r + \lambda)u \tag{3.3}$$

defined in (1.3). We have truncated the infinite domain $\mathbb{R}$ for x to be $\bar{\Omega} = [X_l, X_r]$. A nonuniform mesh $X_l = x_0 < \cdots < x_{m-1} < x_m < x_{m+1} < \cdots < x_M = X_r$ will be used. Let $h_m = x_m - x_{m-1}$ and $h = \frac{X_r - X_l}{M}$. We assume that there exist real numbers δ_0, δ_1, $\delta_2 > 0$ independent of m and M such that the mesh widths satisfy

$$\delta_0 h \le h_m \le \delta_1 h, \quad \text{and} \quad |h_{m+1} - h_m| \le \delta_2 h^2. \tag{3.4}$$

This means that the spatial grid is smooth and quasi-uniform, and the mesh widths h_m tend to zero at the rate of h and vary gradually (see, *e.g.*, [24, 26, 49]).

Based on the above nonuniform grid, the space derivatives of (3.3) are approximated with central finite differences

$$\begin{aligned}
\frac{\partial u}{\partial x}(\tau, x_m) &\approx \frac{u_{m+1}(\tau) - u_{m-1}(\tau)}{h_m + h_{m+1}} := \delta_h u_m(\tau),\\
\frac{\partial^2 u}{\partial x^2}(\tau, x_m) &\approx \frac{2\left[h_m u_{m+1}(\tau) - (h_m + h_{m+1})u_m(\tau) + h_{m+1}u_{m-1}(\tau)\right]}{h_m h_{m+1}(h_m + h_{m+1})}\\
&:= \Delta_h^2 u_m(\tau),
\end{aligned} \tag{3.5}$$

where $u_m(\tau)$ denotes the approximation of $u(\tau, x_m)$. Then the operator $\mathcal{L}$ at (τ, x_m) can be approximated by discrete operator $\mathcal{L}_h$ such as

$$\begin{aligned}
\mathcal{L}_h u_m(\tau) &= \frac{1}{2}\sigma^2\left[\frac{2\left(h_m u_{m+1}(\tau) - (h_m + h_{m+1})u_m(\tau) + h_{m+1}u_{m-1}(\tau)\right)}{h_m h_{m+1}(h_m + h_{m+1})}\right]\\
&\quad + \left(r - \frac{1}{2}\sigma^2 - \lambda\kappa\right)\frac{u_{m+1}(\tau) - u_{m-1}(\tau)}{h_m + h_{m+1}} - (r + \lambda)u_m(\tau)\\
&= \frac{1}{2}\sigma^2\Delta_h^2 u_m(\tau) + \left(r - \frac{1}{2}\sigma^2 - \lambda\kappa\right)\delta_h u_m(\tau) - (r + \lambda)u_m(\tau).
\end{aligned} \tag{3.6}$$

3.3. Approximating integrals

For approximating the integral operator $\mathcal{I}$ in (1.4), we divide the integral term into two parts on Ω and on $\mathbb{R}\setminus\Omega$. By taking into account the asymptotic behaviour of the option, for Merton's model and Kou's model, the integral over $\mathbb{R}\setminus\Omega$

$$R(\tau,x)=\int_{\mathbb{R}\setminus\Omega}u(\tau,x+y)f(y)\mathrm{d}y \tag{3.7}$$

can be computed directly. For European call option, they can be expressed by

$$R(\tau,x)=\begin{cases}S_0e^{x+\mu_{\mathrm{Me}}+\frac{\sigma_{\mathrm{Me}}^2}{2}}\mathcal{N}\left(\frac{x-X_r+\mu_{\mathrm{Me}}+\sigma_{\mathrm{Me}}^2}{\sigma_{\mathrm{Me}}}\right)-Ke^{-r\tau}\mathcal{N}\left(\frac{x-X_r+\mu_{\mathrm{Me}}}{\sigma_{\mathrm{Me}}}\right), & \text{Merton's},\\ S_0\frac{a\eta_1}{\eta_1-1}e^{\eta_1x+(1-\eta_1)X_r}-Kae^{-r\tau+\eta_1(x-X_r)}, & \text{Kou's},\end{cases}$$

and for European put option by

$$R(\tau,x)=\begin{cases}Ke^{-r\tau}\mathcal{N}\left(\frac{X_l-x-\mu_{\mathrm{Me}}}{\sigma_{\mathrm{Me}}}\right)-S_0e^{x+\mu_{\mathrm{Me}}+\frac{\sigma_{\mathrm{Me}}^2}{2}}\mathcal{N}\left(\frac{X_l-x-\mu_{\mathrm{Me}}-\sigma_{\mathrm{Me}}^2}{\sigma_{\mathrm{Me}}}\right), & \text{Merton's},\\ Kbe^{-r\tau+\eta_2(X_l-x)}-S_0\frac{b\eta_2}{\eta_2+1}e^{-\eta_2x+(\eta_2+1)X_l}, & \text{Kou's},\end{cases}$$

where $\mathcal{N}(x)$ is the cumulative normal distribution $\mathcal{N}(x)=\frac{1}{\sqrt{2\pi}}\int_{-\infty}^{x}e^{-\frac{\varsigma^2}{2}}\mathrm{d}\varsigma$ which can be computed directly.

To compute numerically the integral on the region $\Omega:=[X_l,X_r]$, we make the change of variable $y=z-x$, and we obtain

$$\int_{\Omega}u(\tau,x+y)f(y)\mathrm{d}y=\int_{x+X_l}^{x+X_r}u(\tau,z)f(z-x)\mathrm{d}z. \tag{3.8}$$

Let $f_{m,j}:=f(x_j-x_m)$. Then using the composite trapezoidal rule on the interval $\Omega^*=(x+X_l,x+X_r)$, we obtain the following approximation of the integral

$$\int_{\Omega^*}u(\tau,z)f(z-x_m)\mathrm{d}z\approx\frac{1}{2}\left[f_{m,0}u_0h_1+f_{m,M}u_Mh_M+\sum_{j=1}^{M-1}f_{m,j}u_j(h_j+h_{j+1})\right]. \tag{3.9}$$

In view of (3.7)–(3.9), the operator $\mathcal{I}_h$, which approximate the integral operator $\mathcal{I}$, is defined by

$$\begin{aligned}\mathcal{I}_hu_m(\tau)&=\frac{\lambda}{2}\left(u_0(\tau)f_{m,0}h_1+\sum_{j=1}^{M-1}u_j(\tau)f_{m,j}(h_j+h_{j+1})+u_M(\tau)f_{m,M}h_M\right)+\lambda R(\tau,x_m)\\&=\frac{\lambda}{2}F_u+\lambda R(\tau,x_m).\end{aligned} \tag{3.10}$$

3.4. The variable step-sizes IMEX midpoint time discretization

For given positive integers N, $N\geq2$, let the time interval $[0,T]$ be partitioned *via* $J^N:0=\tau_0<\tau_1<\cdots<\tau_N=T$. Let $k_n=\tau_n-\tau_{n-1},\ n=1,2,\ldots,N$, be the time step-sizes which in general will be variable. We set

$$r_n=\frac{k_n}{k_{n-1}},\quad n=2,3,\ldots,N;\quad k_{\max}=\max_{n=1,2,\ldots,N}k_n;\quad r_{\max}=\max_{n=2,\ldots,N}r_n.$$

Let us split the operator $\mathcal{L}$ into the following two parts:

$$\mathcal{L}u(\tau,x)=\mathcal{A}u(\tau,x)+\mathcal{B}u(\tau,x). \tag{3.11}$$

We will treat the operator $\mathcal{A}$ implicitly and the operator $\mathcal{B}$ explicitly. The choices of $\mathcal{A}$ and $\mathcal{B}$ can be different, as studied in [45]. For example, $\mathcal{A}$ ($\mathcal{B} = \mathcal{L} - \mathcal{A}$ accordingly) can be $-\frac{1}{2}\sigma^2\frac{\partial^2}{\partial x^2} + (\vartheta_1 r + \vartheta_2\lambda)I$ with $\vartheta_i \in [0,1]$, $i = 1,2$. As demonstrated in [55], there is no essential difference between the numerical results produced by these different choices. Thus, as a specific example, here we only consider a simple choice:

$$\mathcal{A}u = \frac{1}{2}\sigma^2\frac{\partial^2 u}{\partial x^2} + \left(r - \frac{1}{2}\sigma^2 - \lambda\kappa\right)\frac{\partial u}{\partial x}, \quad \text{and} \quad \mathcal{B}u = -(r+\lambda)u; \tag{3.12}$$

other choices can be treated similarly.

Now let us define $\tilde{\tau}_n = \frac{\tau_{n-1}+\tau_{n+1}}{2}$, the midpoint of the interval $J_n := [\tau_{n-1}, \tau_{n+1}]$. After the time derivation $\frac{\partial u}{\partial t}$ is discretized by midpoint formula,

$$\frac{\partial u}{\partial \tau}(\tilde{\tau}_n, x) \approx \frac{u^{n+1}(x) - u^{n-1}(x)}{k_n + k_{n+1}} := \delta_k u^n(x), \tag{3.13}$$

the fully discrete approximation of option pricing problem (1.1) can be formulated as, for $1 \le n \le N-1$ and $1 \le m \le M-1$

$$\delta_k U_m^n = \mathcal{A}_h\left(\frac{U_m^{n+1} + U_m^{n-1}}{2}\right) + \mathcal{B}_h(EU_m^n) + \mathcal{I}_h(EU_m^n), \tag{3.14}$$

where U_m^n is an approximate value of the solution $u_m^n = u(\tau_n, x_m)$, $EU_m^n = \gamma_{1,n}U_m^n + \gamma_{2,n}U_m^{n-1}$ with

$$\gamma_{1,n} = \frac{k_n + k_{n+1}}{2k_n} = \frac{1}{2}(1 + r_{n+1}), \quad \text{and} \quad \gamma_{2,n} = \frac{k_n - k_{n+1}}{2k_n} = \frac{1}{2}(1 - r_{n+1}).$$

We note that for a uniform time grid, that is, the step-size $k_n \equiv k = T/N$ is a constant, the variable step-size IMEX midpoint scheme (3.14) degenerates to Crank–Nicolson-Leapfrog (CNLF) scheme which applies a scheme somewhat like the Crank–Nicolson to the operator $\mathcal{A}_h$ and a Leapfrog scheme to the operators $\mathcal{I}_h$ and $\mathcal{B}_h$. This constant step-size CNLF scheme has been applied to PIDEs (1.1) in [32]. It is also noteworthy that the scheme (3.14) is different from the variable step-size IMEX linear multistep schemes introduced in [54]. In the scheme (3.14), the operator $\mathcal{B}_h$ can be also treated implicitly.

For the scheme (3.14), the value $U^0 = \left[U_1^0, \ldots, U_{M-1}^0\right]^T$ has been given by the initial condition, and the value $U^1 = \left[U_1^1, \ldots, U_{M-1}^1\right]^T$ will be obtained by IMEX Euler scheme

$$\frac{U_m^1 - U_m^0}{k_1} = \mathcal{A}_h U_m^1 + \mathcal{B}_h U_m^0 + \mathcal{I}_h U_m^0, \quad 1 \le m \le M-1. \tag{3.15}$$

4. Numerical examples

In this section, as did in [55], we proceed by studying numerically the scheme (3.14) and (3.15) for three different cases. The first one concerns European call option under Merton's model, the second one concerns European put option under Merton's model, while in the third one we consider a European put option under Kou's model. In these European options, we note that the initial function

$$g(x) = \phi(e^x) = \begin{cases} (S_0 e^x - K)^+, & \text{in the case of a call option,} \\ (K - S_0 e^x)^+, & \text{in the case of a put option,} \end{cases} \tag{4.1}$$

has a slop discontinuity at $x = \ln(K/S_0)$. To follow the similar forms to those of the previous literature, we take $S_0 = K$.

4.1. Variable space grid

Since the initial function (4.1) has a slop discontinuity at $x = 0$, it is necessary to concentrate grid points near $x = 0$. We use the following variable space grid

$$x(\zeta = 0) = X_l, \quad x(\zeta = 1) = X_r, \quad x(\zeta) = \tilde{x} + \alpha \sin h(a_2\zeta + a_1(1-\zeta)), \tag{4.2}$$

where α is a prescribed uniformity parameter, $x_m := x(\zeta_m)$, $\zeta_m = \frac{m-1}{M}$, $m = 1, 2, \ldots, M+1$, $a_1 = \sin h^{-1}(\frac{X_l - \tilde{x}}{\alpha})$, $a_2 = \sin h^{-1}(\frac{X_r - \tilde{x}}{\alpha})$, and $\tilde{x}$ relates to the slop discontinuity point (therefore $\tilde{x} = 0$ here); see, *e.g.*, [24, 27, 49].

4.2. Two types of variable time grid

In the literature some researchers proposed several types of variable time grid; see, *e.g.*, [7, 36, 50]. Here we consider two of them.

Choice 1 for time grid: $J^{N,1}$. According to [50], this type of grid is accomplished by choosing the approximation times τ_n

$$\tau_n = \begin{cases} \left(\frac{1-\varpi_1^{n/(2N-4)}}{1-\varpi_1}\right) T, & n = 0, 1, 2, 3, \\ \left(\frac{1-\varpi_1^{(n-2)/(N-2)}}{1-\varpi_1}\right) T, & n = 4, 5, \ldots, N, \end{cases} \tag{4.3}$$

where ϖ_1 is a constant greater than one. For this type of grid, the time steps near the expiry $t = T$, *i.e.*, $\tau = 0$, become smaller by increasing ϖ_1.

Choice 2 for time grid: $J^{N,2}$. The second type of grid has been considered in [7]. It is accomplished by choosing the time levels τ_n according to $\tau_n = T(n/N)^{\varpi_2}$ with $\varpi_2 \geq 1$. Observe that $\varpi_2 = 1$ corresponds to constant step-size.

We note that in contrast to the uniform time and space grids, these variable time grids and nonuniform space grid will not increase any complexity and computational costs of the method.

4.3. Example 1: European call option under Merton's model

We first price a European call option and show the convergence order of the IMEX MP method (3.14) and (3.15) with different types of time grid.

It is well-known that when there are no jumps, the option value $V_{BS}(S, \tau)$ can be computed by the Black–Scholes formula:

$$V_{BS}(S, \tau, K, \zeta_n, \sigma_n) = \begin{cases} S\mathcal{N}(d_1) - Ke^{-\zeta_n \tau}\mathcal{N}(d_2), & \text{in the case of a call option,} \\ Ke^{-\zeta_n \tau}\mathcal{N}(-d_2) - S\mathcal{N}(-d_1), & \text{in the case of a put option,} \end{cases}$$

where $\tau \in [0, T]$, $S \in [S_{\min}, S_{\max}]$, $\sigma_n^2 = \sigma^2 + \frac{n\sigma_{\text{Me}}^2}{\tau}$, $\zeta_n = r - \lambda\kappa + \frac{n}{\tau}\left(\mu_{\text{Me}} + \frac{1}{2}\sigma_{\text{Me}}^2\right)$, and

$$d_1 = \frac{\ln\left(\frac{S}{K}\right) + \left(\zeta_n + \frac{\sigma_n^2}{2}\right)\tau}{\sigma_n\sqrt{\tau}}, \quad d_2 = \frac{\ln\left(\frac{S}{K}\right) + \left(\zeta_n - \frac{\sigma_n^2}{2}\right)\tau}{\sigma_n\sqrt{\tau}} = d_1 - \sigma_n\sqrt{\tau}.$$

Based on this Black–Scholes formula, for Merton's model, the price of a European option can be expressed as an infinite sum [38]:

$$V(t, S) = \sum_{n=0}^{\infty} \frac{(\lambda'\tau)^n}{n!} e^{-\lambda'\tau} V_{BS}(S, \tau, K, \zeta_n, \sigma_n), \tag{4.4}$$

where $\tau = T - t$, $\tau \in [0, T]$, and $\lambda' = \lambda(1 + \kappa)$. Then the reference solution can be calculated by the formula (4.4) with the first six terms in the sum from which we can obtain six digits of accuracy in the option price.

TABLE 1. The value of European call option under Merton's model obtained by the variable step-sizes IMEX MP scheme with choice 1 ($\varpi_1 = 4$) and the convergence orders of the scheme. Upper: uniform space grid; bottom: nonuniform space grid.

		$S = 90$		$S = 100$		$S = 110$	
M	N	Error	Order	Error	Order	Error	Order
128	25	2.2424E-03		3.5504E-02		8.0955E-03	
256	50	6.4693E-04	1.7964	8.7638E-03	2.0189	2.0750E-03	1.9660
512	100	1.6499E-04	1.9712	2.1858E-03	2.0034	5.2144E-04	1.9925
1024	200	4.1302E-05	1.9983	5.4625E-04	2.0005	1.3048E-04	1.9987
2048	400	1.0310E-05	2.0026	1.3657E-04	1.9999	3.2621E-05	2.0000
		$S = 90$		$S = 100$		$S = 110$	
M	N	Error	Order	Error	Order	Error	Order
128	25	1.8638E-03		1.2399E-02		3.1587E-03	
256	50	4.6858E-04	1.9919	3.0978E-03	2.0009	7.8977E-04	1.9998
512	100	1.1537E-04	2.0221	7.7580E-04	1.9975	1.9714E-04	2.0022
1024	200	2.8582E-05	2.0130	1.9416E-04	1.9984	4.9233E-05	2.0015
2048	400	7.1109E-06	2.0070	4.8573E-05	1.9991	1.2301E-05	2.0009

Using formula (4.4), the reference values for European call option under Merton's model with the parameters (see, *e.g.*, [19, 29, 32, 55])

$$\sigma = 0.15, \quad r = 0.05, \quad \mu_{\text{Me}} = -0.9, \quad \sigma_{\text{Me}} = 0.45,$$
$$\lambda = 0.1, \quad T = 0.25, \quad K = 100, \quad X_l = -1.5, \quad X_r = 1.5,$$

are 0.52763802 at $S = 90$, 4.39124569 at $S = 100$ and 12.64340583 at $S = 110$. The convergence orders at these points are calculated by

$$\text{Order} = \log_2 \left(E_i^{N,M} / E_i^{2N,2M} \right),$$

where $E_i^{N,M}$ denotes the error computed at the maturity date T and $x = x_i$ with N time sub-intervals and M spatial sub-intervals. In this example, the spatial differential operator $\mathcal{L}$ is split into $\mathcal{A} + \mathcal{B}$ with $\mathcal{B} = -(r + \lambda)I$ being treated explicitly.

Let us choose M and N as did in [19, 29, 32, 55] and choose three different time grids: the first is $J^{N,1}$ with $\varpi_1 = 4$, the second is $J^{N,2}$ with $\varpi_2 = 3$, and the third is $J^{N,2}$ with $\varpi_2 = 4$. The pricing errors and the convergence orders of the variable step-size IMEX MP scheme with three different variable time grids are presented in Tables 1–3. From these numerical results, we observe that the variable step-size IMEX MP scheme is of order two for all three time grids and for both types of space grid, uniform space grid and nonuniform space grid (4.2), where $\alpha = 0.5$. It is worth noting that the numerical errors of the method with space nonuniform grid are smaller than those of space uniform grid for all three cases.

We also consider the discrete l^2 error, where the discrete vector norms $\|x\|_{l^2}$ for a column vector $x = [x_1, x_2, \ldots, x_{M-1}]^T \in \mathbb{R}^{M-1}$ is defined by

$$\|x\|_{l^2} = \left(\sum_{j=1}^{M-1} h_j |x_j|^2 \right)^{1/2}.$$

In Figure 1, we show the times evolution of the discrete l^2 errors of Merton's call option produced by the variable step-size IMEX MP scheme with four different time grids. The discrete l^2 errors of the variable step-sizes IMEX MP scheme on the nonuniform space grid (4.2) are also smaller than those on a uniform space grid.

TABLE 2. The value of European call option under Merton's model obtained by the variable step-sizes IMEX MP scheme with choice 2 ($\varpi_2 = 3$) and the convergence orders of the scheme. Upper: uniform space grid; bottom: nonuniform space grid.

		$S = 90$		$S = 100$		$S = 110$	
M	N	Error	Order	Error	Order	Error	Order
128	25	3.6625E-03		3.4234E-02		8.4596E-03	
256	50	1.0122E-03	1.8553	8.4508E-03	2.0183	2.1627E-03	1.9678
512	100	2.5881E-04	1.9675	2.1062E-03	2.0044	5.4343E-04	1.9927
1024	200	6.5063E-05	1.9921	5.2616E-04	2.0011	1.3601E-04	1.9984
2048	400	1.6289E-05	1.9983	1.3151E-04	2.0003	3.4011E-05	1.9998
		$S = 90$		$S = 100$		$S = 110$	
M	N	Error	Order	Error	Order	Error	Order
128	25	3.2977E-03		1.1187E-02		3.5014E-03	
256	50	8.3420E-04	1.9830	2.7881E-03	2.0045	8.7599E-04	1.9989
512	100	2.0920E-04	1.9955	6.9646E-04	2.0012	2.1903E-04	1.9998
1024	200	5.2345E-05	1.9988	1.7407E-04	2.0003	5.4760E-05	2.0000
2048	400	1.3089E-05	1.9996	4.3516E-05	2.0001	1.3690E-05	2.0000

TABLE 3. The value of European call option under Merton's model obtained by the variable step-sizes IMEX BDF2 scheme with choice 2 ($\varpi_2 = 4$) and the convergence orders of the scheme. Upper: uniform space grid; bottom: nonuniform space grid.

		$S = 90$		$S = 100$		$S = 110$	
M	N	Error	Order	Error	Order	Error	Order
128	25	5.3416E-03		3.2739E-02		8.9121E-03	
256	50	1.4281E-03	1.9032	8.0953E-03	2.0159	2.2630E-03	1.9775
512	100	3.6255E-04	1.9778	2.0184E-03	2.0039	5.6776E-04	1.9949
1024	200	9.0988E-05	1.9945	5.0424E-04	2.0010	1.4205E-04	1.9990
2048	400	2.2770E-05	1.9988	1.2604E-04	2.0002	3.5517E-05	1.9998
		$S = 90$		$S = 100$		$S = 110$	
M	N	Error	Order	Error	Order	Error	Order
128	25	4.9851E-03		9.7648E-03		3.9243E-03	
256	50	1.2506E-03	1.9950	2.4363E-03	2.0029	9.7469E-04	2.0094
512	100	3.1296E-04	1.9985	6.0880E-04	2.0007	2.4326E-04	2.0024
1024	200	7.8270E-05	1.9994	1.5217E-04	2.0003	6.0789E-05	2.0006
2048	400	1.9571E-05	1.9998	3.8041E-05	2.0001	1.5195E-05	2.0002

Example 2: European put option under Merton' model. In this example, we choose the parameters in model as (see, *e.g.*, [28,55])

$$\sigma = 0.3, \quad r = 0, \quad \mu_{\text{Me}} = 0, \quad \sigma_{\text{Me}} = 0.5,$$
$$\lambda = 1.0, \quad T = 0.5, \quad K = 100, \quad X_l = -2, \quad X_r = 2.$$

The reference values for European put option under Merton's model are 20.41168240 at $S = 90$, 15.03495881 at $S = 100$ and 10.95077346 at $S = 110$, which are obtained by the formula (4.4). From the numerical results presented in Table 4, we observe that the variable step-sizes IMEX MP scheme is of order 2 for all four time grids and the errors of the variable step-sizes IMEX MP scheme at the slop discontinuity point $S = K = 100$ are smaller than those of the constant step-size IMEX MP scheme on a uniform space grid.

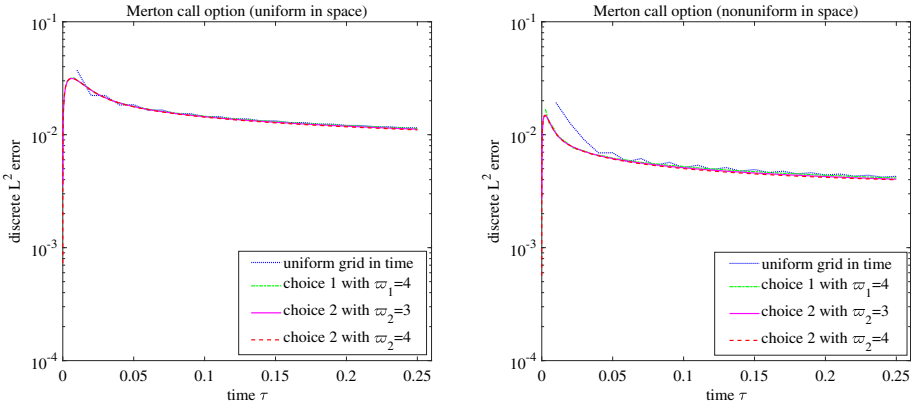

FIGURE 1. The times evolution of the discrete l^2 errors of Merton's call option produced by the variable step-size IMEX MP scheme with four different time grids, where $M = 128$ and $N = 25$. *Left*: uniform gird in space. *Right*: nonuniform grid in space.

TABLE 4. The value of European put option under Merton's model obtained by the variable step-size IMEX MP method on uniform mesh in space. Upper: uniform mesh in time; second: $J^{N,1}$ with $\varpi_1 = 4$; third: $J^{N,2}$ with $\varpi_2 = 3$; bottom: $J^{N,2}$ with $\varpi_2 = 4$.

		$S = 90$		$S = 100$		$S = 110$	
M	N	Error	Order	Error	Order	Error	Order
128	25	1.3858E-02		1.7903E-02		1.6983E-02	
256	50	3.0245E-03	2.1960	3.9037E-03	2.1973	4.0705E-03	2.0608
512	100	7.3292E-04	2.0450	1.0213E-03	1.9344	1.0066E-03	2.0157
1024	200	1.6018E-04	2.1940	2.4593E-04	2.0541	2.3180E-04	2.1185
2048	400	1.7011E-05	3.2352	4.6059E-05	2.4167	3.8128E-05	2.6040
128	25	1.2138E-02		1.5721E-02		1.6373E-02	
256	50	3.0050E-03	2.0141	3.9037E-03	2.0098	4.0367E-03	2.0201
512	100	7.3129E-04	2.0388	9.6812E-04	2.0116	9.9913E-04	2.0144
1024	200	1.6017E-04	2.1908	2.2446E-04	2.1087	2.3014E-04	2.1182
2048	400	1.7057E-05	3.2312	3.6468E-05	2.6218	3.7741E-05	2.6083
128	25	1.0107E-02		1.2668E-02		1.5165E-02	
256	50	2.4749E-03	2.0299	3.1120E-03	2.0253	3.7355E-03	2.0214
512	100	5.9251E-04	2.0625	7.5237E-04	2.0483	9.1035E-04	2.0368
1024	200	1.2471E-04	2.2483	1.6615E-04	2.1790	2.0732E-04	2.1346
2048	400	8.0970E-06	3.9450	2.0045E-05	3.0512	3.1957E-05	2.6977
128	25	7.8259E-03		9.1784E-03		1.3775E-02	
256	50	1.8756E-03	2.0609	2.2113E-03	2.0533	3.3647E-03	2.0335
512	100	4.3867E-04	2.0961	5.2198E-04	2.0828	8.1315E-04	2.0489
1024	200	8.5745E-05	2.3550	1.0788E-04	2.2746	1.8245E-04	2.1560
2048	400	1.7082E-06	5.6495	5.3941E-06	4.3219	2.5667E-05	2.8295

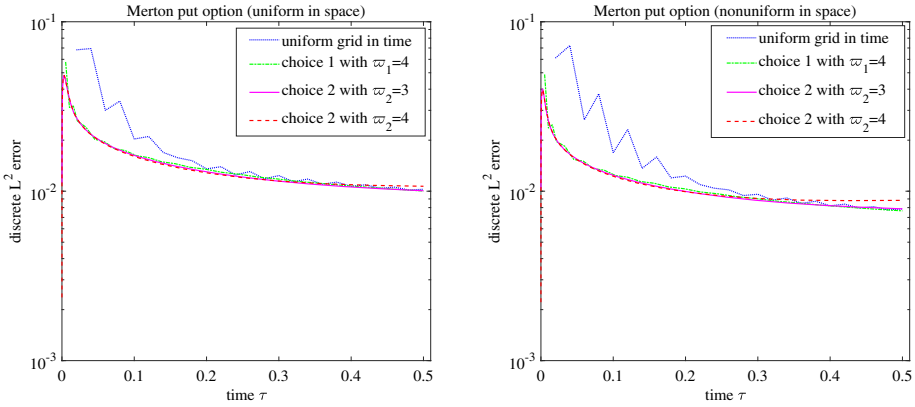

FIGURE 2. The times evolution of the discrete l^2 errors of Merton's put option produced by the variable step-size IMEX MP scheme with four different time grids, where $M = 128$ and $N = 25$. *Left*: uniform gird in space. *Right*: nonuniform grid in space.

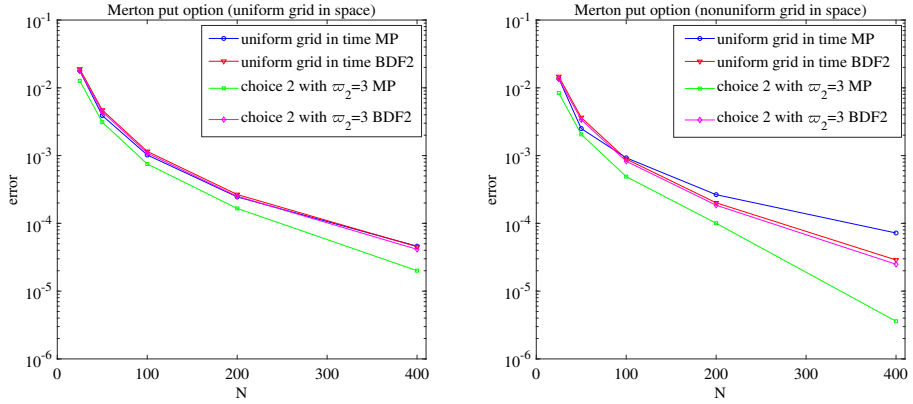

FIGURE 3. Errors at $S = K$ of Merton's put option produced by two variable step-size IMEX schemes with two different time grids. *Left*: uniform gird in space. *Right*: nonuniform grid in space.

The time evolution of the discrete l^2 errors of the numerical results on $[0, 0.5]$ are shown in Figure 2. For the nonuniform space mesh, we take $\alpha = 2$. From Figure 2, we find that the numerical errors of the constant step-size IMEX MP scheme will be oscillating on both the uniform and nonuniform space grids. The numerical results also reveal that the variable step-size IMEX MP method has much smaller errors (especially near $\tau = 0$) than the constant step-size IMEX MP method.

To compare the variable step-size IMEX MP scheme with the variable step-size IMEX BDF2 scheme discussed in [55], in Figure 3, we show the errors at $S = K$ of Merton's put option produced by the two schemes with two different time grids and two different space grids. The results suggest that the errors of the two variable-step schemes at the singular point on nonuniform space grid are smaller than those on uniform space grid. From Figure 3, we also observe that for variable spatial grid, the errors of the variable step-size IMEX MP scheme at $S = K$ are slightly smaller than those of the variable step-size IMEX BDF2 scheme.

TABLE 5. CPU times of the two variable step-sizes IMEX schemes, MP and BDF2, with choice 1 ($\varpi_2 = 4$) on nonuniform grid in space for European put option under Merton's model.

		CPU time (s)	
M	N	IMEX MP	IMEX BDF2
128	25	0.049	0.051
256	50	0.117	0.120
512	100	0.439	0.441
1024	200	2.781	2.797
2048	400	27.289	28.115

To illustrate the effectiveness of the two variable step-size schemes, we also present their CPU times in second in Table 5. It will be observed that the distinction between the two schemes is not sharp; the CPU times of the variable step-size MP scheme are slightly less than those of the variable step-size BDF2 scheme.

Example 3: European put option under Kou's model. In the final numerical example, we consider pricing a European put option under Kou's model. As did in [19, 28, 32, 44, 55], the parameters in model are chosen as

$$\sigma = 0.15, \quad r = 0.05, \quad a = 0.3445, \quad \eta_1 = 3.0465, \quad \eta_2 = 3.0775,$$
$$\lambda = 0.1, \quad T = 0.25, \quad K = 100, \quad X_l = -1.5, \quad X_r = 1.5.$$

Since the reference values for European put option under Kou's model can not obtained by an analytical formula similar to (4.4), we compute the convergence order by using the double grid principle

$$\text{Order} = \log_2 \frac{\|U^{N,M} - U^{2N,2M}\|_{l_2}}{\|U^{2N,2M} - U^{4N,4M}\|_{l_2}},$$

where $U^{N,M}$ represents the numerical solution at T with N time sub-intervals and M spatial sub-intervals. Let us choose M and N as did in [19, 29, 32, 55].

The discrete l^2 errors of the two variable step-size IMEX schemes, MP (3.14) and BDF2 discussed in [55], for the case of $\mathcal{B} \equiv 0$ are listed in Tables 6 (uniform space grid) and 7 (non-uniform space grid). The numerical results show the errors have the second-order convergence accuracy for both numerical schemes and for all four time grids and two space grids, and there is little, if any, difference between the numerical data produced by the two IMEX schemes. As a matter of fact, this is also true for other choices of $\mathcal{A}$ and $\mathcal{B}$. It is to be expected that the errors of the two variable step-sizes IMEX schemes, MP and BDF2 schemes, are smaller than those of the corresponding constant step-size IMEX schemes.

In order to compare farther the computational efficiency of the two IMEX schemes, MP and BDF2, we list the CPU times of the two variable step-size IMEX schemes in Table 8. We still observe that the CPU times of the variable step-size MP scheme are very slightly less than those of the variable step-size BDF2 scheme when the time-space grid is refined.

5. STABILITY ANALYSIS FOR THE SCHEME

To explain the behavior of the numerical solutions obtained by the fully discrete scheme (3.14) and (3.15), we should theoretically analyze the potential advantages of this scheme. In this section, we first investigate the stability of the IMEX midpoint finite difference scheme (3.14) by using the Von Neumann analysis.

To show the stability, we first need the following lemma.

Lemma 5.1. *A variable step-size finite difference scheme for a scalar equation is stable if all the roots, $g_v(\theta)$, of the amplification polynomial $G(\theta, k_n, h_m)$ satisfy the following conditions:*

TABLE 6. The discrete l^2 error of the two variable step-size IMEX schemes, MP and BDF2 schemes, for European put option under Kou's model on uniform grid in space. Upper: uniform mesh in time; second: $J^{N,1}$ with $\varpi_1 = 4$; third: $J^{N,2}$ with $\varpi_2 = 3$; bottom: $J^{N,2}$ with $\varpi_2 = 4$.

		MP		BDF2	
M	N	$\|U^{N,M} - U^{2N,2M}\|_{l_2}$	Order	$\|U^{N,M} - U^{2N,2M}\|_{l_2}$	Order
256	50	8.5434E-03		8.5659E-03	
512	100	2.0795E-03	2.0386	2.1243E-03	2.0116
1024	200	5.1889E-04	2.0027	5.3004E-04	2.0028
2048	400	1.2966E-04	2.0007	1.3244E-04	2.0007
4096	800	3.2412E-05	2.0002	3.3107E-05	2.0002
256	50	8.3339E-03		8.3402E-03	
512	100	2.0680E-03	2.0108	2.0711E-03	2.0097
1024	200	5.1637E-04	2.0017	5.1705E-04	2.0020
2048	400	1.2907E-04	2.0002	1.2923E-04	2.0004
4096	800	3.2269E-05	2.0000	3.2308E-05	2.0000
256	50	8.1789E-03		8.1944E-03	
512	100	2.0298E-03	2.0106	2.0316E-03	2.0120
1024	200	5.0655E-04	2.0026	5.0676E-04	2.0032
2048	400	1.2658E-04	2.0006	1.2661E-04	2.0009
4096	800	3.1642E-05	2.0002	3.1645E-05	2.0003
256	50	8.0151E-03		8.0568E-03	
512	100	1.9895E-03	2.0104	1.9943E-03	2.0143
1024	200	4.9650E-04	2.0025	4.9708E-04	2.0043
2048	400	1.2407E-04	2.0006	1.2414E-04	2.0015
4096	800	3.1014E-05	2.0002	3.1023E-05	2.0006

(i) *There is a constant* C' *such that* $|g_v| \leq 1 + C' k_{\max}$.
(ii) *There is a constant* C_k *such that* $k_{\max} \leq C_k T/N$.
(iii) *There are positive constants* c_0 *and* c_1 *such that if* $c_0 \leq |g_v| \leq 1 + C' k_{\max}$, *then* $|g_v|$ *is a simple root, and for any other root* g_u *the relation*

$$|g_v - g_u| \geq c_1$$

holds for h *and* $k_{\max}$ *sufficiently small.*

Additionally, the conditions (i) *and* (iii) *are the necessary conditions for the stability of a variable step-size finite difference scheme for a scalar equation.*

Proof. In the case of the constant step-size numerical methods, it is well known that the conditions (i) and (iii) are the sufficient and necessary conditions for the stability of a finite difference scheme for a scalar equation (see, *e.g.*, [48], Thm. 4.2.2). As a consequence, we only need to show the stability under the conditions (i), (ii) and (iii). In fact, in this case, we have

$$|g_v|^N \leq (1 + C' k_{\max})^N \leq (1 + C' C_k T/N)^N \leq e^{C' C_k T},$$

and thus the scheme is stable. □

The condition (ii) implies that the time grid is quasi-uniform and the ratio r_n of consecutive step-sizes should be bounded. For the two types of grid exploited in Section 4, we now show that they satisfy condition (ii). For $J^{N,1}$, let $\psi_N := \varpi_1^{\frac{1}{2N-4}}$. It has been verified in [55] that $k_1 = \frac{1-\psi_N}{1-\varpi_1}$, $k_n = \psi_N^{n-1} k_1$, $n = 2, 3, 4,$

TABLE 7. The discrete l^2 error of the variable step-size IMEX MP method for European put option under Kou's model on nonuniform grid in space. Upper: uniform mesh in time; second: $J^{N,1}$ with $\varpi_1 = 4$; third: $J^{N,2}$ with $\varpi_2 = 3$; bottom: $J^{N,2}$ with $\varpi_2 = 4$.

		MP		BDF2	
M	N	$\|U^{N,M} - U^{2N,2M}\|_{l_2}$	Order	$\|U^{N,M} - U^{2N,2M}\|_{l_2}$	Order
256	50	3.2557E-03		3.2786E-03	
512	100	7.7099E-04	2.0782	8.1708E-04	2.0045
1024	200	1.9262E-04	2.0010	2.0409E-04	2.0012
2048	400	4.8145E-05	2.0003	5.1010E-05	2.0004
4096	800	1.2036E-05	2.0001	1.2752E-05	2.0001
256	50	3.0503E-03		3.0567E-03	
512	100	7.6059E-04	2.0038	7.6374E-04	2.0008
1024	200	1.9032E-04	1.9987	1.9100E-04	1.9995
2048	400	4.7606E-05	1.9992	4.7765E-05	1.9995
4096	800	1.1905E-05	1.9995	1.1944E-05	1.9997
256	50	2.9250E-03		2.9414E-03	
512	100	7.2935E-04	2.0037	7.3125E-04	2.0081
1024	200	1.8222E-04	2.0010	1.8244E-04	2.0030
2048	400	4.5546E-05	2.0003	4.5571E-05	2.0012
4096	800	1.1386E-05	2.0001	1.1389E-05	2.0005
256	50	2.8252E-03		2.8656E-03	
512	100	7.0381E-04	2.0051	7.0878E-04	2.0154
1024	200	1.7579E-04	2.0013	1.7640E-04	2.0065
2048	400	4.3938E-05	2.0003	4.4011E-05	2.0029
4096	800	1.0984E-05	2.0001	1.0992E-05	2.0014

TABLE 8. CPU times of the two variable step-size IMEX schemes, MP and BDF2, for European put option under Kou's model.

		CPU time (s)	
M	N	IMEX MP	IMEX BDF2
128	25	0.405	0.397
256	50	1.004	1.019
512	100	3.533	3.570
1024	200	14.252	14.371
2048	400	76.552	77.823

and $k_n = \psi_N^{2(n-3)}(1+\psi_N)k_1$, $n = 5, 6, \ldots, N$. Then we know that the time grid is quasi-uniform, that is, $k_{\max} \le \varpi_1(1+\varpi_1)T/N$. As for the grid $J^{N,2}$, it is easy to verify that $k_n = \tau_n - \tau_{n-1} \le 2\varpi_2 T/N$ and therefore the condition (ii) is satisfied.

We now follow the approach of [32] and multiply both sides of the equation in (3.14) by $2\tilde{k}_n := k_n + k_{n+1}$ and rewrite it in the form

$$
\begin{aligned}
-\alpha_1\frac{\tilde{k}_n}{2}U_{m+1}^{n+1} + \left(1+\alpha_2\frac{\tilde{k}_n}{2}\right)U_m^{n+1} - \alpha_3\frac{\tilde{k}_n}{2}U_{m-1}^{n+1} &= \alpha_1\frac{\tilde{k}_n}{2}U_{m+1}^{n-1} + \left(1-\alpha_2\frac{\tilde{k}_n}{2}\right)U_m^{n-1} + \alpha_3\frac{\tilde{k}_n}{2}U_{m-1}^{n-1} \\
&\quad + 2\tilde{k}_n\mathcal{B}_h(EU_m^n) + \lambda\tilde{k}_n(EF_U^n) + 2\gamma_{1,n}\lambda\tilde{k}_n R(\tau_n, x_m) \\
&\quad + 2\gamma_{2,n}\lambda\tilde{k}_n R(\tau_{n-1}, x_m), \qquad (5.1)
\end{aligned}
$$

where

$$\alpha_1 = \frac{2\sigma^2}{h_{m+1}(h_m + h_{m+1})} + \frac{2}{h_m + h_{m+1}}\left(r - \frac{1}{2}\sigma^2 - \lambda\kappa\right),$$
$$\alpha_2 = \frac{2\sigma^2}{h_m h_{m+1}},$$
$$\alpha_3 = \frac{2\sigma^2}{h_m(h_m + h_{m+1})} - \frac{2}{h_m + h_{m+1}}\left(r - \frac{1}{2}\sigma^2 - \lambda\kappa\right).$$

When we use the Von Neumann analysis to derive the amplification polynomial of the finite difference method in (5.1), the last two terms in (5.1) will be neglected because they are free from U_m^n. Let us replace U_m^n in the scheme by $g^n e^{im\theta}$ for each n and m and cancel the factor $g^{n-1}e^{im\theta}$. Then we have the amplification polynomial $G(\theta, k_n, h_m)$, which is defined by

$$G(\theta, k_n, h_m) = \beta_2 g^2 - 2\beta_1 g - \beta_0, \tag{5.2}$$

where

$$\beta_0 = 1 - \frac{\sigma^2}{h_m h_{m+1}}\tilde{k}_n(1 - \cos\theta) + i\left[\frac{2\tilde{k}_n}{h_m + h_{m+1}}\left(r - \frac{1}{2}\sigma^2 - \lambda\kappa\right) - \frac{\sigma^2(h_m - h_{m+1})}{h_m h_{m+1}(h_m + h_{m+1})}\tilde{k}_n\right]\sin\theta + 2\gamma_{2,n}\lambda\tilde{k}_n(F_R + iF_I) - 2\gamma_{2,n}\tilde{k}_n(r + \lambda),$$
$$\beta_1 = -\gamma_{1,n}\tilde{k}_n(r + \lambda) + \gamma_{1,n}\lambda\tilde{k}_n(F_R + iF_I),$$
$$\beta_2 = 1 + \frac{\sigma^2}{h_m h_{m+1}}\tilde{k}_n(1 - \cos\theta) - i\left[\frac{2\tilde{k}_n}{h_m + h_{m+1}}\left(r - \frac{1}{2}\sigma^2 - \lambda\kappa\right) - \frac{\sigma^2(h_m - h_{m+1})}{h_m h_{m+1}(h_m + h_{m+1})}\tilde{k}_n\right]\sin\theta,$$

with F_R and F_I being real numbers such that

$$F_R + iF_I = \frac{1}{2}\left(f_{m,0}e^{-im\theta}h_1 + \sum_{j=1}^{M-1} f_{m,j}e^{i(j-m)\theta}(h_j + h_{j+1}) + f_{m,M}e^{i(M-m)\theta}h_M\right).$$

As a consequence of the above analysis, we have the following stability theorem.

Theorem 5.2 (Stability). *If $k_{\max}$ and $r_{\max}$ satisfy the condition*

$$k_{\max}(1 + r_{\max})^2 < \frac{2}{r + 2\lambda}, \tag{5.3}$$

and there is a constant C_k such that $k_{\max} \le C_k T/N$, then the finite difference method (3.14) is stable in the sense of the Von Neumann analysis.

Proof. After considerable algebra, we find that

$$|\beta_2| > 1, \quad |\beta_1| < \frac{1}{4}(r + 2\lambda)k_n(1 + r_{n+1})^2, \quad |\beta_0/\beta_2| < 1 + (r + 2\lambda)k_n\left|1 - r_{n+1}^2\right|.$$

Let g be a root of the amplification polynomial $G(\theta, k_n, h_m)$. Then we have

$$\begin{aligned}|g| &= \left|\frac{2\beta_1/\beta_2 \pm \sqrt{4\beta_1^2/\beta_2^2 + 4\beta_0/\beta_2}}{2}\right| \\ &\le 2|\beta_1/\beta_2| + |\sqrt{\beta_0/\beta_2}| \\ &\le 1 + \frac{1}{4}(r+2\lambda)k_n\left[(1+r_{n+1})^2 + 4|1-r_{n+1}^2|\right].\end{aligned}$$

The remainder of this proof is similar to that of Theorem 6.3 in [32]. Let g_1 and g_2 be two roots of $G(\theta, k_n, h_m) = 0$. If $g_1 > 1$ (in this case $c_0 = 1$), then

$$\begin{aligned}|g_1 - g_2| = |2g_1 - (g_1+g_2)| &\ge 2|g_1| - |g_1+g_2| \\ &\ge 2 - \frac{1}{2}(r+2\lambda)k_n(1+r_{n+1})^2.\end{aligned}$$

Using condition (5.3), we have

$$|g_1 - g_2| \ge 1.$$

In this case $c_1 = 1$. This proves (iii) in Lemma 5.1 and completes the proof. □

For the constant step-size MP method, the condition (5.3) becomes $k_{\max} < \frac{1}{2(r+2\lambda)}$, which has been obtained in [32]; see similar results in [46]. From the condition (5.3), we find that the larger the admissible step-size $k_{\max}$, the smaller the admissible step-size ratio $r_{\max}$ will be. It is worth mentioning that a similar conclusion has been reached for the variable step-size IMEX BDF2 method in [55]. Then we conjecture that this interesting property is exclusive for the variable step-size IMEX multistep numerical schemes.

6. Error estimates for the scheme (3.14) and (3.15)

In this section we will derive the consistency error and the global error bounds for the scheme (3.14) and (3.15). To do this, we need to analyze the regularity of the solutions to the option problem (2.8) and (2.9).

6.1. Regularity of solutions

Due to the non-smoothness of the payoff function g, singularities may arise at $\tau = 0$. Nevertheless, one finds that it is continuous on $\mathbb{R}$ and satisfies the following assumption:

Assumption 6.1. *There exist $\zeta_1, \ldots, \zeta_P \in \mathbb{R}$ such that g is C^∞ on (ζ_j, ζ_{j+1}) for $j = 1, \ldots, P-1$ and for all $l \ge 0$, for all $x \notin \{\zeta_1, \ldots, \zeta_P\}$, $|g^{(l)}(x)| < C_g$ with a constant C_g depending on g.*

Based on these findings, Cont and Voltchkova in [16] proved the following L^∞ regularity of the solutions.

Lemma 6.2 (L^∞-regularity, [16])**.** *Let g be continuous on $\mathbb{R}$ and verify Assumption 6.1. Then, for all $\tau > 0$ and $l, p \in \mathbb{N}$, $l + p > 0$, the viscosity solution $U(\tau, x)$ of the problem (2.8) and (2.9) satisfies*

$$\left\|\frac{\partial^{l+p}U}{\partial\tau^l\partial x^p}(\tau,\cdot)\right\|_{L^\infty} \le C\tau^{-l-(p-1)/2}, \tag{6.1}$$

where the constant C depends only on l, p, C_g, T, and the coefficient of the operators $\mathcal{L}$ and $\mathcal{I}$ (σ, r, λ and κ).

6.2. Consistency

In this subsection, using Lemma 6.2, we derive the consistency error of the scheme (3.14) and (3.15). For this purpose, we assume that there exists a constant C_I independent of τ such that the integral operator $\mathcal{I}$ satisfies the condition

$$\|\mathcal{I}(u)\|_{L^\infty} \le C_I \|u\|_{L^\infty}. \tag{6.2}$$

It is easy to verify that condition (6.2) is satisfied for finite activity jump-diffusion model, *i.e.*, $\nu(\mathbb{R}) = \lambda < \infty$, (*e.g.*, Merton's model and Kou's model). For simplicity, we define the discrete operator $\mathcal{L}_h^*$ as

$$\mathcal{L}_h^* U_m^n = \begin{cases} \mathcal{A}_h U_m^n + \mathcal{B}_h U_m^{n-1}, & n = 1, \quad 1 \le m \le M-1, \\ \mathcal{A}_h \left(\frac{U_m^{n+1} + U_m^{n-1}}{2} \right) + \mathcal{B}_h (E U_m^n), & n \ge 2, \quad 1 \le m \le M-1. \end{cases} \tag{6.3}$$

Then the consistency error d_m^n of the scheme (3.14) and (3.15) for the solution u of (1.1) and (1.2), *i.e.*, the amounts by which the exact solution misses satisfying (3.14) and (3.15), is given by, for $2 \le n \le N$ and $1 \le m \le M-1$,

$$d_m^n = \frac{\partial u}{\partial \tau}(\tilde{\tau}_n, x_m) - \mathcal{L}u(\tilde{\tau}_n, x_m) - \mathcal{I}_h u(\tilde{\tau}_n, x_m) - [\delta_k u_m^n - \mathcal{L}_h^* u_m^n - \mathcal{I}_h (E u_m^n)] \tag{6.4}$$

and, for $n = 1$ and $1 \le m \le M-1$,

$$d_m^1 = \frac{\partial u}{\partial \tau}(\tau_1, x_m) - \mathcal{L}u_m^1 - \mathcal{I}u_m^1 - \left[\frac{u_m^1 - u_m^0}{k_1} - \mathcal{L}_h^* u_m^1 - \mathcal{I}_h u_m^0 \right], \tag{6.5}$$

where $u_m^n := u(\tau_n, x_m)$. We also define the discrete vector norm $\|x\|_{l^\infty}$ of a given column vector $x = [x_1, x_2, \ldots, x_{M-1}]^T \in \mathbb{R}^{M-1}$ as

$$\|x\|_{l^\infty} = \max_{1 \le j \le M-1} |x_j|.$$

The corresponding operator matrix norm $\|A\|_p$ ($p = 2, \infty$) is defined, by

$$\|A\|_p = \max_{x \ne 0} \frac{\|Ax\|_{l^p}}{\|x\|_{l^p}}.$$

Then we have the following theorems.

Theorem 6.3 (Consistency error of scheme (3.14))**.** *Let g be continuous on $\mathbb{R}$ and verify Assumption 6.1, the integral operator $\mathcal{I}$ satisfy (6.2), $r_{\max}$ be bounded, and the spatial grid be smooth, i.e., satisfy (3.4). Then for sufficient small $k_{\max}$ and h, we have, for $2 \le n \le N$ and $1 \le m \le M$,*

$$|d_m^n| \le C \left[\left(\tau_{n-1}^{-5/2} + \tau_{n-1}^{-2} + \tau_{n-1}^{-3/2} + 1 \right) k_n^2 + \left(\tau_{n-1}^{-3/2} + \tau_{n-1}^{-1} + \tau_{n-1}^{-1/2} \right) h^2 \right], \tag{6.6}$$

where $(\tilde{\tau}_n, x_m) \in (0, T] \times (X_l, X_r)$.

Proof. To prove (6.6), we first consider

$$\begin{aligned} |d_m^n| &\le \left| \frac{\partial u}{\partial \tau}(\tilde{\tau}_n, x_m) - \delta_k u_m^n \right| + |\mathcal{L}u(\tilde{\tau}_n, x_m) - \mathcal{L}_h^* u_m^n| + |\mathcal{I}_h u(\tilde{\tau}_n, x_m) - \mathcal{I}_h (E u_m^n)| \\ &= I_1 + I_2 + I_3. \end{aligned} \tag{6.7}$$

For the first term I_1, using Taylor's expansion and Lemma 6.2, we obtain

$$I_1 \le \frac{(k_n+k_{n+1})^2}{24} \sup_{\tau\in J_n}\left|\frac{\partial^3 u}{\partial \tau^3}(\tau, x_m)\right| \le C\tau_{n-1}^{-5/2}k_n^2, \tag{6.8}$$

where $J_n = [\tau_{n-1}, \tau_{n+1}]$ has been introduced in Section 3.4.

Let us look at the second term I_2:

$$I_2 \le |\mathcal{A}u(\tilde{\tau}_n, x_m) - \mathcal{A}_h\tilde{u}(\tau_n, x_m)| + |\mathcal{B}u(\tilde{\tau}_n, x_m) - \mathcal{B}_h(Eu_m^n)| = I_{21} + I_{22}, \tag{6.9}$$

where $\tilde{u}(\tau_n, x_m) = \frac{u_m^{n+1}+u_m^{n-1}}{2}$. Then we have

$$\begin{aligned} I_{21} \le \frac{\sigma^2}{2}&\left|\frac{\partial^2 u}{\partial x^2}(\tilde{\tau}_n, x_m) - \frac{\partial^2 \tilde{u}}{\partial x^2}(\tau_n, x_m) + \frac{\partial^2 \tilde{u}}{\partial x^2}(\tau_n, x_m) - \frac{1}{2}\left(\Delta_h^2 u_m^{n+1} + \Delta_h^2 u_m^{n-1}\right)\right| \\ &+ \left|\frac{\sigma^2}{2} - r + \lambda\kappa\right|\left|\frac{\partial u}{\partial x}(\tilde{\tau}_n, x_m) - \frac{\partial \tilde{u}}{\partial x}(\tau_n, x_m)\right. \\ &\left. + \frac{\partial \tilde{u}}{\partial x}(\tau_n, x_m) - \frac{1}{2}\left(\delta_h u_m^{n+1} + \delta_h u_m^{n+1}\right)\right|. \end{aligned} \tag{6.10}$$

In view of the regularity estimate (6.1), we have

$$\begin{aligned} \left|\frac{\partial^l u}{\partial \tau^l}(\tilde{\tau}_n, x_m) - \frac{\partial^l \tilde{u}}{\partial \tau^l}(\tau_n, x_m)\right| &\le \frac{(k_n+k_{n+1})^2}{8} \sup_{\tau\in J_n}\left|\frac{\partial^{l+2} u}{\partial \tau^2 \partial x^l}(\tau, x_m)\right| \\ &\le C\tau_{n-1}^{-2-(l-1)/2}k_n^2, \quad l = 1, 2, \end{aligned} \tag{6.11}$$

and, in view of the smoothness of the spatial grid,

$$\begin{aligned} \left|\frac{\partial^2 u}{\partial x^2}(\tau_{n\pm1}, x_m) - \Delta_h^2 u_m^{n\pm1}\right| &\le \frac{|h_{m+1}-h_m|}{6}\left\|\frac{\partial^3 u}{\partial x^3}(\tau_{n\pm1}, \cdot)\right\|_{L^\infty} + \frac{\left|h_{m+1}^2 - h_m h_{m+1} + h_m^2\right|}{12}\left\|\frac{\partial^4 u}{\partial x^4}(\tau_{n\pm1}, \cdot)\right\|_{L^\infty} \\ &\le C\left(h^2\tau_{n\pm1}^{-1} + h^2\tau_{n\pm1}^{-3/2}\right). \end{aligned} \tag{6.12}$$

Similarly, we obtain

$$\begin{aligned} \left|\frac{\partial u}{\partial x}(\tau_{n\pm1}, x_m) - \delta_h u_m^{n\pm1}\right| &\le \frac{|h_{m+1}-h_m|}{2}\left\|\frac{\partial^2 u}{\partial x^2}(\tau_{n\pm1}, \cdot)\right\|_{L^\infty} + \frac{\left|h_{m+1}^2 - h_m h_{m+1} + h_m^2\right|}{6}\left\|\frac{\partial^3 u}{\partial x^3}(\tau_{n\pm1}, \cdot)\right\|_{L^\infty} \\ &\le C\left(h^2\tau_{n\pm1}^{-1/2} + h^2\tau_{n\pm1}^{-1}\right). \end{aligned} \tag{6.13}$$

Substitute (6.11)–(6.13) into (6.10) to obtain

$$I_{21} \le C\left[\left(\tau_{n-1}^{-5/2} + \tau_{n-1}^{-2}\right)k_n^2 + \left(\tau_{n-1}^{-3/2} + \tau_{n-1}^{-1} + \tau_{n-1}^{-1/2}\right)h^2\right]. \tag{6.14}$$

For I_{22}, an application of Lemma 6.2 and Taylor's formula yields

$$\begin{aligned} \left|u(\tilde{\tau}_n, x_m) - \left(\gamma_{1,n}u_m^n + \gamma_{2,n}u_m^{n-1}\right)\right| &\le \frac{|k_n^2 - k_{n+1}^2|}{8} \sup_{\tau\in J_n}\left|\frac{\partial^2 u}{\partial \tau^2}(\tau, x_m)\right| \\ &\le C\tau_{n-1}^{-3/2}k_n^2. \end{aligned} \tag{6.15}$$

Combining (6.14) and (6.15), we bound I_2 as follows

$$I_2 \le C\left[\left(\tau_{n-1}^{-5/2} + \tau_{n-1}^{-2} + \tau_{n-1}^{-3/2}\right)k_n^2 + \left(\tau_{n-1}^{-3/2} + \tau_{n-1}^{-1} + \tau_{n-1}^{-1/2}\right)h^2\right]. \tag{6.16}$$

We now direct our attention to estimate I_3. It follows from (3.10) that

$$I_3 \le \left| \int_{\Omega^*} u(\tilde{\tau}_n, z) f(z - x_m) \mathrm{d}z - \frac{\lambda}{2}(EF_u^n) \right| + \left| R(\tilde{\tau}_n, x_m) - \gamma_{1,n} R(\tau_n, x_m) - \gamma_{2,n} R(\tau_{n-1}, x_m) \right|. \tag{6.17}$$

Taking the expression $R(\tau, x)$ for European option into account, we easily estimate the second term on the right hand of (6.17) as follows

$$\left| R(\tilde{\tau}_n, x_m) - \gamma_{1,n} R(\tau_n, x_m) - \gamma_{2,n} R(\tau_{n-1}, x_m) \right| \le C k_n^2.$$

Using Taylor's expansion we have, in view of (6.2),

$$\begin{aligned}
&\left| \int_{\Omega^*} u(\tilde{\tau}_n, z) f(z - x_m) \mathrm{d}z - \gamma_{1,n} \int_{\Omega^*} u(\tau_n, z) f(z - x_m) \mathrm{d}z - \gamma_{2,n} \int_{\Omega^*} u(\tau_{n-1}, z) f(z - x_m) \mathrm{d}z \right| \\
&\le \frac{|k_n^2 - k_{n+1}^2|}{8} \sup_{\tau \in J_n} \left| \int_{\Omega^*} \frac{\partial^2 u}{\partial \tau^2}(\tau, z) f(z - x_m) \mathrm{d}z \right| \\
&\le C \tau_{n-1}^{-3/2} k_n^2.
\end{aligned}$$

With the composite trapezoidal rule over the interval Ω^*, we get

$$\begin{aligned}
\left| \int_{\Omega^*} u(\tau_{n-j}, z) f(z - x_m) \mathrm{d}z - \frac{1}{2} F_u^{n-j} \right| &\le \frac{M}{12} \sum_{i=1}^{M} h_i^3 \left\| \frac{\partial^2 u}{\partial z^2}(\tau_{n-j}, \cdot) \right\|_{L^\infty} \\
&\le C h^2 \tau_{n-j}^{-1/2}, \quad j = 0, 1 \quad i = 1, \ldots, M.
\end{aligned}$$

As a consequence of the above analysis, we have the following estimate for I_3

$$I_3 \le C \left(\tau_{n-1}^{-3/2} k_n^2 + k_n^2 + h^2 \tau_{n-1}^{-1/2} \right) \quad i = 1, \ldots, M. \tag{6.18}$$

Combining (6.8), (6.16), and (6.18), we obtain the required estimate (6.6) and thus complete the proof. □

Since the low regularity of the exact solution at $\tau = 0$, we are a little more focused on the error behavior for $\tau_{n-1} < 1$. In this case, the estimate for d_m^n can be simplified as

$$|d_m^n| \le C \left(\tau_{n-1}^{-5/2} k_n^2 + \tau_{n-1}^{-3/2} h^2 \right). \tag{6.19}$$

The following theorem provides an estimate for the consistency error of the scheme (3.15).

Theorem 6.4 (Consistency error of scheme (3.15))**.** *Let g be continuous on $\mathbb{R}$ and verify Assumption 6.1, the integral operator $\mathcal{I}$ satisfy (6.2), and the spatial grid be smooth, i.e., satisfy (3.4). Then for $k_1 < 1$ and $h < 1$, we have*

$$\left| d_m^1 \right| \le C \left[k_1^{-1/2} + h^2 k_1^{-3/2} \right], \quad 1 \le m \le M - 1. \tag{6.20}$$

Proof. Using Taylor's expansion and Lemma 6.2, we have

$$\begin{aligned}
\left| \frac{\partial u}{\partial \tau}(\tau_1, x_m) - \frac{u_m^1 - u_m^0}{k_1} \right| &= \left| \frac{1}{k_1} \int_0^{\tau_1} \tau u''(\tau, x_m) \mathrm{d}\tau \right| \le \frac{1}{k_1} \int_0^{\tau_1} \tau \left\| u''(\tau, \cdot) \right\|_{L^\infty} \mathrm{d}\tau \\
&\le \frac{1}{k_1} \int_0^{\tau_1} \tau^{-1/2} \mathrm{d}\tau = 2 k_1^{-1/2}.
\end{aligned} \tag{6.21}$$

Similarly, we estimate the error $\mathcal{A}u_m^1 - \mathcal{A}_h u_m^1$ by

$$\begin{aligned}
\left|\mathcal{A}u_m^1 - \mathcal{A}_h u_m^1\right| \le{}& \frac{|h_{m+1}^2 - h_m h_{m+1} + h_m^2|}{12}\frac{\sigma^2}{2}\left\|\frac{\partial^4 u}{\partial x^4}(\tau_1,\cdot)\right\|_{L^\infty} \\
&+\frac{|h_{m+1}-h_m|}{6}\frac{\sigma^2}{2}\left\|\frac{\partial^3 u}{\partial x^3}(\tau_1,\cdot)\right\|_{L^\infty} \\
&+\frac{|h_{m+1}^2 - h_m h_{m+1} + h_m^2|}{6}\left|\frac{\sigma^2}{2} - r + \lambda\kappa\right|\left\|\frac{\partial^3 u}{\partial x^3}(\tau_1,\cdot)\right\|_{L^\infty} \\
&+\frac{|h_{m+1}-h_m|}{2}\left|\frac{\sigma^2}{2} - r + \lambda\kappa\right|\left\|\frac{\partial^2 u}{\partial x^2}(\tau_1,\cdot)\right\|_{L^\infty} \\
\le{}& C\left[h^2\left(k_1^{-3/2} + k_1^{-1}\right) + h^2\left(k_1^{-1} + k_1^{-1/2}\right)\right] \\
\le{}& Ch^2 k_1^{-3/2}.
\end{aligned} \tag{6.22}$$

The reaction term can be estimated as follows

$$\left|\mathcal{B}u_m^1 - \mathcal{B}_h u_m^0\right| \le (r+\lambda)k_1\left\|\frac{\partial u}{\partial \tau}(\tau_1,\cdot)\right\|_{L^\infty} \le Ck_1. \tag{6.23}$$

The integral part can be bounded by

$$\begin{aligned}
\left|\mathcal{I}u_m^1 - \mathcal{I}_h u_m^0\right| \le{}& \frac{\lambda}{12}\sum_{i=1}^{M} h_i^3\left\|\frac{\partial^2 u}{\partial x^2}(\tau_{n-j},\cdot)\right\|_{L^\infty} + \lambda\int_0^{\tau_1}\left\|\frac{\partial u}{\partial \tau}(\tau,\cdot)\right\|_{L^\infty}\mathrm{d}\tau \\
\le{}& C\left(\int_0^{\tau_1}\tau^{-1/2}\mathrm{d}\tau + h^2\right) \le C(k_1^{1/2} + h^2). \quad i = 1,\ldots,M.
\end{aligned} \tag{6.24}$$

Assembling the various terms and using the fact that $k_1 < 1$ and $h < 1$ we obtain (6.20). □

We observe that the consistency errors d_m^n, $n \ge 1$, are affected by the regularity of the solution u, especially, the approximation of time derivative $\frac{\partial u}{\partial \tau}(\tau, x_m)$.

6.3. Error estimates

Now we derive the error estimates for the IMEX MP finite difference method. Let the error at (τ_n, x_m) be

$$E_m^n = u_m^n - U_m^n \quad \text{for} \quad 0 \le m \le M,$$

and the error vector E^n be defined by $E^n := [E_1^n, E_2^n, \ldots, E_{M-1}^n]^T$. We are ready to give the error estimates for the variable step-size IMEX MP method.

Theorem 6.5 (Error estimates)**.** *Let $u(\tau, x)$ be the exact solution to the initial-valued PIDE (1.1) and (1.2), and let U_m^n be the numerical solution to PIDE (1.1) and (1.2) obtained by the variable step-size IMEX midpoint method (3.14) with the IMEX Euler method (3.15) for the starting value U_m^1. If $k_{\max} \le C_k T/N$ and the spatial grid is smooth, i.e., satisfies (3.4), then the error E^n $(n = 2, 3, \ldots, N)$ satisfies*

$$\|E^n\|_{l^2} \le C\left[k_1^{1/2} + h^2 k_1^{-1/2} + \sum_{j=2}^{n-1}\tilde{k}_j\left(\left(\tau_{j-1}^{-5/2} + 1\right)k_j^2 + \left(\tau_{j-1}^{-3/2} + \tau_{j-1}^{-1/2}\right)h^2\right)\right], \tag{6.25}$$

where the constant C is independent of the time step-sizes k_j and the space mesh diameter h.

Proof. The idea of the proof stems from [32]. By the definition (6.4) on the consistency error d_m^n of the scheme (3.14), using (5.1), we obtain the error equation for $1 \le n \le N-1$ and $1 \le m \le M-1$

$$\left(I + \frac{\tilde{k}_n}{2}B\right) E^{n+1} = \left(I - \frac{\tilde{k}_n}{2}B\right) E^{n-1} + A_n E^{n-1} + C_n E^n + \tilde{k}_n d^n, \tag{6.26}$$

where I is the identity matrix of size $M-1$, and $A_n := (a_{mj}^n)$, $B := (b_{mj})$ and $C_n := (c_{mj}^n)$ are square matrices of size $M-1$ with entries

$$a_{mj}^n = \begin{cases} -2\gamma_{2.n}(r+\lambda)\tilde{k}_n + 2\gamma_{2,n}\lambda\tilde{k}_n f_{m,j}, & \text{for} \quad j = m, \quad 1 \le m \le M-1, \\ 2\gamma_{2,n}\lambda\tilde{k}_n f_{m,j}, & \text{for} \quad j \ne m, \quad 1 \le m \le M-1, \end{cases}$$

$$b_{mj} = \begin{cases} -\alpha_3 & \text{for} \quad j = m-1, \quad 2 \le m \le M-1, \\ \alpha_2 & \text{for} \quad j = m, \quad 1 \le m \le M-1, \\ -\alpha_1 & \text{for} \quad j = m+1, \quad 1 \le m \le M-2, \\ 0 & \text{otherwise}, \end{cases}$$

$$c_{mj}^n = \begin{cases} -2\gamma_{1,n}(r+\lambda)\tilde{k}_n + 2\gamma_{1,n}\lambda\tilde{k}_n f_{m,j}, & \text{for} \quad j = m, \quad m \le j \le M-1, \\ 2\gamma_{1,n}\lambda\tilde{k}_n f_{m,j}, & \text{for} \quad j \ne m, \quad 1 \le m \le M-1, \end{cases}$$

and $d^n := (d_m^n) \in \mathbb{R}^{M-1}$ with entries d_m^n satisfying (6.6). It is clear that the matrix $(I + \frac{\tilde{k}_n}{2}B)$ with the sufficiently small h is nonsingular for it is strictly diagonally dominated. Then multiplying both sides of (6.26) by $\left(I + \frac{\tilde{k}_n}{2}B\right)^{-1}$ and taking the discrete l^2 norm yield

$$\begin{aligned} \|E^{n+1}\|_{l^2} \le & \left\| \left(I + \frac{\tilde{k}_n}{2}B\right)^{-1} \left(I - \frac{\tilde{k}_n}{2}B\right) \right\|_2 \|E^{n-1}\|_{l^2} \\ & + \left\| \left(I + \frac{\tilde{k}_n}{2}B\right)^{-1} A_n \right\|_2 \|E^{n-1}\|_{l^2} \\ & + \left\| \left(I + \frac{\tilde{k}_n}{2}B\right)^{-1} C_n \right\|_2 \|E^n\|_{l^2} + \left\| \left(I + \frac{\tilde{k}_n}{2}B\right)^{-1} \right\|_2 \tilde{k}_n \|d^n\|_{l^2}. \end{aligned} \tag{6.27}$$

With the same arguments as in [32], we can show

$$\left\| \left(I + \frac{\tilde{k}_n}{2}B\right)^{-1} \left(I - \frac{\tilde{k}_n}{2}B\right) \right\|_2 \le 1, \tag{6.28}$$

and

$$\left\| \left(I + \frac{\tilde{k}_n}{2}B\right)^{-1} \right\|_2 \le 1. \tag{6.29}$$

Since matrix A_n is a square Toeplitz matrix, using the estimates (6.29) and $|\lambda_j(A_n)| \le \|A_n\|_\infty$, we have

$$\begin{aligned}\left\| \left(I + \frac{\tilde{k}_n}{2} B\right)^{-1} A_n \right\|_2 &\le \|A_n\|_2 = \sqrt{\lambda_{\max}(A_n^T A_n)} \le \sqrt{\|A_n^T A_n\|_\infty} \\ &\le \sqrt{\|A_n^T\|_\infty \|A_n\|_\infty} \le \|A_n\|_\infty \\ &\le \frac{1}{2}(r + 2\lambda) k_n |1 - r_{n+1}^2|. \end{aligned} \tag{6.30}$$

Similarly, we get

$$\left\| \left(I + \frac{\tilde{k}_n}{2} B\right)^{-1} C_n \right\|_2 \le \|C_n\|_2 \le \frac{1}{2}(r + 2\lambda) k_n (1 + r_{n+1})^2. \tag{6.31}$$

Substitute (6.28)–(6.31) into (6.27) to obtain

$$\begin{aligned}\|E^{n+1}\|_{l^2} &\le \|E^{n-1}\|_{l^2} + \frac{1}{2}(r + 2\lambda) k_n |1 - r_{n+1}^2| \|E^{n-1}\|_{l^2} \\ &\quad + \frac{1}{2}(r + 2\lambda) k_n (1 + r_{n+1})^2 \|E^n\|_{l^2} + \tilde{k}_n \|d^n\|_{l^2} \\ &\le \left[1 + \frac{1}{2}(r + 2\lambda) k_n (1 + r_{n+1})^2\right] \|E^{n-1}\|_{l^2} \\ &\quad + \frac{1}{2}(r + 2\lambda) k_n (1 + r_{n+1})^2 \|E^n\|_{l^2} + \tilde{k}_n \|d^n\|_{l^2}. \end{aligned} \tag{6.32}$$

Adding $\|E^n\|_{l^2}$ into both sides of (6.32), we obtain, by induction,

$$\begin{aligned}\|E^{n+1}\|_{l^2} + \|E^n\|_{l^2} &\le \left[1 + \frac{1}{2}(r + 2\lambda) k_n (1 + r_{n+1})^2\right] \left(\|E^n\|_{l^2} + \|E^{n-1}\|_{l^2}\right) + \tilde{k}_n \|d^n\|_{l^2} \\ &\le \prod_{j=1}^{n} \left[1 + \frac{1}{2}(r + 2\lambda) k_j (1 + r_{j+1})^2\right] \left(\|E^1\|_{l^2} + \|E^0\|_{l^2}\right) \\ &\quad + \sum_{j=1}^{n} \prod_{i=j+1}^{n} \left[1 + \frac{1}{2}(r + 2\lambda) k_i (1 + r_{i+1})^2\right] \tilde{k}_j \|d^j\|_{l^2}. \end{aligned}$$

Replacing n by $n - 1$, with $\|E^0\|_{l^2} = 0$, we further have

$$\begin{aligned}\|E^n\|_{l^2} &\le \prod_{j=1}^{n-1} \left[1 + \frac{1}{2}(r + 2\lambda) k_j (1 + r_{j+1})^2\right] \|E^1\|_{l^2} \\ &\quad + \sum_{j=1}^{n-1} \prod_{i=j+1}^{n-1} \left[1 + \frac{1}{2}(r + 2\lambda) k_i (1 + r_{i+1})^2\right] \tilde{k}_j \|d^j\|_{l^2} \\ &\le e^{(r+2\lambda)(1+r_{\max})^2 \tau_{n-1}/2} \|E^1\|_{l^2} + \sum_{j=1}^{n-1} e^{(r+2\lambda)(1+r_{\max})^2 (\tau_{n-1} - \tau_{j+1})/2} \tilde{k}_j \|d^j\|_{l^2} \\ &\le C \|E^1\|_{l^2} + C \sum_{j=1}^{n-1} \tilde{k}_j \|d^j\|_{l^2}. \end{aligned} \tag{6.33}$$

Using the estimate (6.20) for the consistency error d_m^1 of the IMEX Euler method, we can bound the error $\|E^1\|_{l^2}$ as

$$\|E^1\|_{l^2} \leq C\left(k_1^{1/2} + h^2 k_1^{-1/2}\right). \tag{6.34}$$

Substituting (6.34) and (6.6) into (6.33), we obtain (6.25) and therefore the desired result. This completes the proof. □

When we assume that $T < 1$, the global error estimate (6.25) can be rewritten as

$$\|E^n\|_{l^2} \leq C\left[k_1^{1/2} + h^2 k_1^{-1/2} + \sum_{j=2}^{n-1} \tilde{k}_j \left(\tau_{j-1}^{-5/2} k_j^2 + \tau_{j-1}^{-3/2} h^2\right)\right]. \tag{6.35}$$

From (6.25) or (6.35), we observe that due to the non-smoothness of the initial data $g(x)$, it is beneficial to take smaller time steps near $\tau = 0$. These error estimates suggest that the time step-sizes k_n should be scaled as $k_n \leq h^2$ for small n, *e.g.*, $n = 1, 2, 3, 4$, and $k_n = O(h)$ for large n. Numerical results presented in Section 4 confirm our theoretical findings.

7. Concluding remarks

The non-smoothness of the payoff function g in the jump-diffusion option pricing model may leads to singularities of the solution at $\tau = 0$. To resolve the low regularity of the solution at the slop discontinuity point $S = K$ and at $\tau = 0$, we use variable time step-size IMEX methods with nonuniform space grid for solving this type of equations and take smaller space steps near the slop discontinuity point $S = K$ and smaller time steps near $\tau = 0$. Since the variable time step-size IMEX methods allow us take different time step-sizes for different time scales, variable step-sizes are often essential to obtain computationally efficient, accurate results for solutions of time dependent differential equation with different time scales. In [55], by using energy method, we investigated the stability and error estimates of the variable step-size IMEX BDF2 method. In this work, we continued studying the variable step-size IMEX numerical methods for European option pricing model and combined the techniques used in the literature. As a consequence, we proved the stability of the variable step-sizes IMEX MP method, which can be viewed as a variable step-size extension of CNLF scheme, a three time level scheme considered in [32], in the sense of the Von Neumann analysis. We also derived the consistency error and the global error bounds of this method based on the regularity results obtained in [16]. The theoretical and numerical results obtained in this paper for European option pricing models show that step-size ratios of the variable step-size MP method are not subject to a constant upper bound such as the variable step-size BDF2 method, and further demonstrate the prominent advantages of high accuracy compared to the constant step-size IMEX methods. Applying these efficient variable step-size IMEX methods to American option pricing models (see, *e.g.*, [8, 30, 33]) will be our future work.

In this paper, the error was estimated under l^2-norm. From a financial point of view, it is also important to estimate the l^∞ error or the quantization error [49], which may lead to serious degradation in the convergence rates of numerical schemes. The quantization error has been analyzed for numerical methods for the Black–Scholes equation described by a convection-diffusion equation (see, *e.g.*, [14, 21]). It is a interest topic of further research to extend the analysis of quantization error to the IMEX schemes for PIDEs (1.1) and (1.2).

Acknowledgements. The authors would like to thank the anonymous referees for comments and suggestions that led to improvements in the presentation of this paper. This work was supported by National Natural Science Foundation of China (Grant No. 11771060) and by Shanghai Science and Technology Planning Projects (Grant No. 20JC1414200), sponsored by Natural Science Foundation of Shanghai (Grant No. 20ZR1441200).

References

[1] Y. Achdou and O. Pironneau, Computational Methods for Option Pricing. In: Vol. 30 of *Frontiers in Applied Mathematics*. SIAM, Philadelphia, PA (2005).

[2] G. Akrivis, M. Crouzeix and C. Makridadis, Implicit–explicit multistep finite element methods for nonlinear parabolic equations, Report 95-22, University of Rennes (1995).

[3] A. Almendral and C.W. Oosterlee, Numerical valuation of options with jumps in the underlying. *Appl. Numer. Math.* **53** (2005) 1–18.

[4] L. Andersen and J. Andreasen, Jump-diffusion processes: volatility smile fitting and numerical methods for option pricing. *Rev. Deriv. Res.* **4** (2000) 231–262.

[5] U.M. Ascher, S.J. Ruuth and B.T.R. Wetton, Implicit–explicit methods for time-dependent PDE's. *SIAM J. Numer. Anal.* **32** (1995) 797–823.

[6] U.M. Ascher, S.J. Ruuth and R.J. Spiteri, Implicit–explicit Runge–Kutta methods for time-dependent partial differential equations. *Appl. Numer. Math.* **25** (1997) 151–167.

[7] J. Becker, A second order backward difference method with variable steps for a parabolic problem. *BIT* **38** (1998) 644–662.

[8] L. Boen and K.J. in 't Hout, Operator splitting schemes for American options under the two-asset Merton jump-diffusion model. Preprint arXiv:1912.06809 (2019).

[9] L. Boen and K.J. in 't Hout, Operator splitting schemes for the two-asset Merton jump-diffusion model. *J. Comput. Appl. Math.* **387** (2021) 112309.

[10] M. Briani, R. Natalini and G. Russo, Implicit–explicit numerical schemes for jump-diffusion processes. *Calcolo* **44** (2007) 33–57.

[11] W. Chen, X. Wang, Y. Yan and Z. Zhang, A second order BDF numerical scheme with variable steps for the Cahn–Hilliard equation. *SIAM J. Numer. Anal.* **57** (2019) 495–525.

[12] Y.Z. Chen, W.S. Wang and A.G. Xiao, An efficient algorithm for options under Merton's jump-diffusion model on nonuniform grids. *Comput. Econ.* **48** (2018) 1–27.

[13] Y.Z. Chen, A.G. Xiao and W.S. Wang, An IMEX-BDF2 compact scheme for pricing options under regime-switching jump-diffusion models. *Math. Methods Appl. Sci.* **42** (2019) 2646–2663.

[14] C.C. Christara and N.C. Leung, Analysis of quantization error in financial pricing via finite difference methods. *SIAM J. Numer. Anal.* **56** (2018) 1731–1757.

[15] R. Cont and P. Tankov, Financial Modelling with Jump Processes. Chapman & Hall/CRC, Boca Raton, FL (2004).

[16] R. Cont and E. Voltchkova, A finite difference scheme for option pricing in jump diffusion and exponential lévy models. *SIAM J. Numer. Anal.* **43** (2005) 1596–1624.

[17] M. Crouzeix, Une méthode multipas implicite-explicite pour l'approximation des équations d'évolution paraboliques. *Numer. Math.* **35** (1980) 257–276.

[18] Y. d'Halluin, P.A. Forsyth and G. Labahn, A penalty method for American options with jump diffusion processes. *Numer. Math.* **97** (2004) 321–352.

[19] Y. d'Halluin, P.A. Forsyth and K.R. Vetzal, Robust numerical methods for contingent claims under jump diffusion processes. *IMA J. Numer. Anal.* **25** (2005) 87–112.

[20] L. Feng and V. Linetsky, Pricing options in jump-diffusion models: an extrapolation approach. *Oper. Res.* **56** (2008) 304–325.

[21] P.A. Forsyth and K.R. Vetzal, Quadratic convergence for valuing American options using a penalty method. *SIAM J. Sci. Comput.* **23** (2002) 2095–2122.

[22] J. Frank, W. Hundsdorfer and J.G. Verwer, On the stability of implicit–explicit linear multistep methods. *Appl. Numer. Math.* **25** (1997) 193–205.

[23] B. Gaviraghi, M. Annunziato and A. Borzía, Analysis of splitting methods for solving a partial integro-differential Fokker–Planck equation. *Appl. Math. Comput.* **294** (2017) 1–17.

[24] K.J. in 't Hout, Numerical Partial Differential Equations in Finance Explained: An Introduction to Computational Finance. Springer Nature, London (2017).

[25] K.J. in 't Hout and J. Toivanen, ADI schemes for valuing European options under the Bates model. *Appl. Numer. Math.* **130** (2018) 143–156.

[26] K.J. in 't Hout and K. Volders, Stability and convergence analysis of discretizations of the Black–Scholes PDE with the linear boundary condition. *IMA J. Numer. Anal.* **34** (2014) 296–325.

[27] M.K. Kadalbajoo, L.P. Tripathi and A. Kumar, Second order accurate IMEX methods for option pricing under Merton and Kou jump-diffusion model. *J. Sci. Comput.* **65** (2015) 979–1024.

[28] M.K. Kadalbajoo, A. Kumar and L.P. Tripathi, An efficient numerical method for pricing options under jump diffusion model. *Int. J. Adv. Eng. Sci. Appl. Math.* **7** (2015) 114–123.

[29] M.K. Kadalbajoo, A. Kumar and L.P. Tripathi, A radial basis function based implicit–explicit method for option pricing under jump-diffusion models. *Appl. Numer. Math.* **110** (2016) 159–173.

[30] M.K. Kadalbajoo, L.P. Tripathi and A. Kumar, An error analysis of a finite element method with IMEX-time semidiscretizations for some partial integro-differential inequalities arising in the pricing of American options. *SIAM J. Numer. Anal.* **55** (2017) 869–891.

[31] S.G. Kou, A jump diffusion model for option pricing. *Manage. Sci.* **48** (2002) 1086–1101.

[32] Y. Kwon and Y. Lee, A second-order finite difference method for option pricing under jump-diffusion models. *SIAM J. Numer. Anal.* **49** (2011) 2598–2617.

[33] Y. Kwon and Y. Lee, A second-order tridiagonal method for American options under jump-diffusion models. *SIAM J. Sci. Comput.* **33** (2011) 1860–1872.

[34] S.T. Lee and H.W. Sun, Fourth order compact scheme with local mesh refinement for option pricing in jump-diffusion model. *Numer. Methods Part. Differ. Equ.* **28** (2012) 1079–1098.

[35] H.L. Liao, T. Tang and T. Zhou, On energy stable, maximum-principle preserving, second order BDF scheme with variable steps for the Allen–Cahn equation. *SIAM J. Numer. Anal.* **58** (2020) 2294–2314.

[36] A.M. Matache, C. Schwab and T.P. Wihler, Fast numerial solution of parabolic integro-differential equations with applications in finance, IMA preprint series 1954, University of Minnesota (2004).

[37] A.M. Matache, T. von Petersdorff and C. Schwab, Fast deterministic pricing of options on Lévy driven assets. *ESAIM: M2AN* **38** (2004) 37–71.

[38] R.C. Merton, Option pricing when underlying stock returns are discontinuous. *J. Fin. Econ.* **3** (1976) 125–144.

[39] D. Nualart and W. Schoutens, Backward stochastic differential equations and Feynman-Kac formula for Lévy processes, with applications in finance. *Bernoulli* **7** (2001) 761–776.

[40] E. Pindza, K.C. Patidar and E. Ngounda, Robust spectral method for numerical valuation of European options under Merton's jump-diffusion model. *Numer. Methods Part. Differ. Equ.* **30** (2014) 1169–1188.

[41] J.A. Rad and K. Parand, Pricing American options under jump-diffusion models using local weak form meshless techniques. *Int. J. Comput. Math.* **94** (2016) 1–27.

[42] J.A. Rad and K. Parand, Numerical pricing of American options under two stochastic factor models with jumps using a meshless local Petrov–Galerkin method. *Appl. Numer. Math.* **115** (2017) 252–274.

[43] S.J. Ruuth, Implicit–explicit methods for reaction-diffusion problems in pattern-formation. *J. Math. Biol.* **34** (1995) 148–176.

[44] S. Salmi and J. Toivanen, An iterative method for pricing American options under jump-diffusion models. *Appl. Numer. Math.* **61** (2011) 821–831.

[45] S. Salmi and J. Toivanen, IMEX schemes for pricing options under jump-diffusion models. *Appl. Numer. Math.* **84** (2014) 33–45.

[46] S. Salmi, J. Tovianen and L. von Sydow, An IMEX-scheme for pricing options under stochastic volatility models with jumps. *SIAM J. Sci. Comput.* **36** (2014) B817–B834.

[47] K. Sato, Lévy Processes and Infinitely Divisible Distributions. Cambridge University Press, Cambridge, UK (1999).

[48] J.C. Strikwerda, Finite Difference Schemes and Partial Differential Equations. SIAM, Philadelphia (2004).

[49] D. Tavella and C. Randall, Pricing Financial Instruments: The Finite Difference Method. John Wiley & Sons, Chichester, UK (2000).

[50] J. Toivanen, Numerical valuation of Europen and American options under Kou's jump-diffusion model. *SIAM J. Sci. Comput.* **4** (2008) 1949–1970.

[51] J.M. Varah, Stability restrictions on second order, three-level finite-difference schemes for parabolic equations. *SIAM J. Numer. Anal.* **17** (1980) 300–309.

[52] J.G. Verwer, J.G. Blom and W. Hundsdorfer, An implicit–explicit approach for atmospheric transport-chemistry problems. *Appl. Numer. Math.* **20** (1996) 191–209.

[53] W.S. Wang and Y.Z. Chen, Fast numerical valuation of options with jump under Merton's model. *J. Comput. Appl. Math.* **318** (2017) 79–92.

[54] D. Wang and S.J. Ruuth, Variable step-size implicit–explicit linear multistep methods for time-dependent partial differential equations. *J. Comput. Math.* **26** (2008) 838–855.

[55] W.S. Wang, Y.Z. Chen and H. Fang, On the variable two-step IMEX BDF method for parabolic integro-differential equations with nonsmooth initial data arising in finance. *SIAM J. Numer. Anal.* **57** (2019) 1289–1317.

[56] W.S. Wang, M.L. Mao and Z. Wang, Stability and error estimates for the variable step-size BDF2 method for linear and semilinear parabolic equations. *Adv. Comput. Math.* **47** (2021) 1–28.

[57] X.L. Zhang, Numerical analysis of American option pricing in a jump-diffusion model. *Math. Oper. Res.* **22** (1997) 668–690.

[58] K. Zhang and S. Wang, A computational scheme for options under jump-diffusion processes. *Int. J. Numer. Anal. Model.* **6** (2009) 110–123.